DISCOVERING MECHANISMS THAT REGULATE BETA-CELL NEOGENESIS AND PROLIFERATION

by
Hannah Elizabeth Edelman

A dissertation submitted to Johns Hopkins University in conformity with the requirements for the degree of Doctor of Philosophy

Baltimore, Maryland
November 2018

ABSTRACT

In both Type I and Type II diabetes, a loss of functioning beta cells results in an inability to produce insulin effectively to regulate blood glucose. Current treatments have a variety of problems including insulin-dependence, donor scarcity, comorbidities, and cost. We are interested in inducing the body to produce its own beta cells endogenously by either neogenesis from progenitors or proliferation of existing beta cells. From previous work, we know that the transcription factor Sox9b plays an important role in the identity of endocrine progenitor cells in the zebrafish pancreas, known as centroacinar cells (CACs), that contribute to regeneration of beta cells. Since humans also have CACs but do not regenerate efficiently, we wanted to understand the downstream targets of Sox9b/SOX9 and their role in the biology of CACs. Using RNA-seq and ChIP-seq in PANC-1 cells we were able to find direct targets of SOX9, including the interesting candidate *EPCAM*, to follow up on. For assessing beta-cell proliferation, we knew from a previous screen that selective serotonin reuptake inhibitors (SSRIs) can induce beta-cell proliferation in the larval zebrafish. We hypothesized that innervation of the principal islet was responsible for this serotonergic signaling to the pancreas. Using imaging of a variety of transgenic lines, we established that innervation of the islet occurs by 4 days post fertilization and that the *sox10* mutant zebrafish has a reduced amount of this innervation. When treated with the SSRI paroxetine (Paxil), we saw that *sox10* mutant fish still had an increase in beta-cell proliferation (compared to DMSO control). This suggests that innervation is in fact not necessary for serotonergic signaling to the pancreas and there must be another source of serotonin production and transport. Our better understanding of both the molecular mechanisms behind CAC differentiation into

new beta cells and the proliferation of beta cells induced by serotonin signaling will help inform new and better treatments of diabetes.

Readers: Michael Parsons, PhD and Jeff Mumm, PhD

ACKNOWLEDGEMENTS

A big thank you to Sarah McClymont, Rebecca Beer, PhD, and Frazer Matthews for their help with data collection and analysis in the collaborative effort described in Part I.

TABLE OF CONTENTS

LIST OF FIGURES

Part I: Investigating the transcriptional targets of SOX9

Part II: Determining the role of islet innervation in serotonergic signaling to the pancreas

LIST OF TABLES

INTRODUCTION

Diabetes is a world-wide health issue – as of 2013, 382 million people suffer from the disease, presenting a huge burden on economic and healthcare systems.[1] The downstream health issues of the hyperglycemia induced by diabetes include serious problems like diabetic ketoacidosis, retinopathy and neuropathy, kidney disease, heart disease, and a general decrease in lifespan.[1] Both Type I and Type II diabetes are diseases of hyperglycemia caused by the dysregulation of blood sugar control. Normally, the beta cells of the pancreas respond to a post-prandial increase in blood sugar by releasing insulin. Insulin acts on other tissues in the body to decrease blood glucose – it stops adipocytes from lipolysis, stops the liver from gluconeogenesis, and induces muscle tissue to take up sugar from the blood for storage.[2] Type I diabetes is an autoimmune disease in which beta cells are destroyed early on in life and therefore patients require an outside source of insulin in order to control their blood sugar.[3] In Type II diabetes, tissues develop insulin resistance and in later stages there is also a loss of functional beta cells.[2,4] Therefore in both cases, a treatment is needed that increases beta-cell mass so that patients are not insulin-dependent.

The first and most widely-used treatment when there is a loss of beta cells is injectable insulin. This is generally managed through a basal injection of long-acting insulin and then multiple bolus injections of shorter-acting insulin after meals.[5] Delivery of exogenous insulin can also be achieved using an insulin pump, where a pump is worn continuously and insulin is received by a subcutaneous cannula. While exogenous insulin does prevent hyperglycemia, it requires patients to either receive multiple injections per day or constantly wear an insulin pump.[6] In addition, determining when to receive insulin

(and how much to receive) means a lot of education of patients (and their parents in the case of children with Type I diabetes) and requires patients to stay engaged in their treatment for a lifetime. If too much insulin is received, it can cause serious hypoglycemia. Finally, exogenous insulin is not a "cure" for diabetes in that patients still do not have enough functioning beta cells.

In order to try to prevent dependence on exogenous insulin, transplants of either the whole pancreas from a donor or of just islet cells (from multiple donors) are becoming more common. With both options, patients can become insulin independent, although this is more common when transplanting the whole pancreas. Although these treatments offer a more sustainable "cure" to loss of beta cells than insulin injections, they come with their own difficulties. First and foremost, transplantation comes with a donor scarcity problem, especially in the case of islet cells which need to come from multiple deceased donors to treat one patient. In addition, transplantation requires lifelong immunosuppression and the surgeries themselves have associated morbidity, especially for whole-organ transplantation.[7,8]

Finally, there is research moving towards using stem-cell derived beta cells as a treatment for diabetes. The company ViaCyte is using human embryonic stem cell-derived pancreatic endoderm (hES-PE) within a microencapsulation device that can be implanted subcutaneously. This device allows for the flow of glucose in and insulin out, but prevents entrance of immune cells so immunosuppression is not required. The hES-PE includes beta-cell-like cells that can respond to blood sugar effectively in mice.[9,10] These devices are currently in human clinical trials but are having difficulty with successful engraftment.

Because each of the current treatment options for beta-cell loss has a range of challenges, the optimal way to treat the beta-cell loss associated with diabetes would be to induce the body to endogenously make more beta cells. This would result in insulin independence, as well as avoid the morbidities associated with transplantation and the cost of differentiating stem cells. Neogenesis, the production of new beta cells from progenitor cells, and proliferation of existing beta cells are two ways in which the body can increase beta-cell mass. In order to induce the endogenous creation of more beta cells, we need to better understand the pathways behind neogenesis and proliferation.

The zebrafish is an excellent model system for studying the mechanisms driving beta-cell neogenesis and proliferation. The morphology of the adult zebrafish pancreas is very similar to that of mammals. Both have the acinar cells of the exocrine pancreas (responsible for synthesizing and secreting digestive enzymes) organized in acini. Ducts, lined by ductal cells, carry these enzymes to the gut. A subset of duct cells known as centroacinar cells (CACs), which will be discussed in more detail in Part I, exist in both zebrafish and mammals.[11] Islets of endocrine cells, including beta cells, exist between acini – these islets, like in humans, have a core of beta cells surrounded by alpha, delta, and epsilon cells.[12] The larval zebrafish pancreas also has these same cell types – acinar cells, ductal cells, and endocrine cells (organized in the principal and secondary islets).[11]

Similar molecular pathways also exist in the zebrafish and mammalian pancreas. The development of the mammalian and zebrafish pancreas involves very similar stages – specification of pancreas from foregut endoderm by transcription factors like *PTF1A* and *PDX1* and involvement of the FGF10 and Notch signaling pathways in fate determination, for example.[13,14] Ductal cells express SOX9 (or Sox9b) in both the

mammalian and zebrafish pancreas.[15-17] In addition, RNA-seq work comparing the transcriptomes of pancreatic cells in zebrafish, mice, and humans found that there are overlapping core groups of genes that determine the identity and functions of endocrine cells in all three species.[18] Because of the similar morphology and molecular underpinnings of the pancreas in zebrafish compared to mammals, we can use the zebrafish to study the mechanisms behind beta-cell neogenesis and proliferation to find better treatment strategies for increasing beta-cell mass.

PART I: Investigating the transcriptional targets of SOX9

INTRODUCTION

Ultimately, both Type I and Type II diabetes result in a loss of functioning beta-cells. Current treatments, including insulin injections, transplantation of donor beta cells, and differentiation of stem cells are compromised by systemic complications, scarcity of donor tissues, and cost, respectively. An effective treatment for these diseases would ideally involve an increase in beta-cell mass. Thus exploring the induction of beta-cells endogenously from pancreatic progenitors is an alluring treatment target. However, the capacity for beta-cell neogenesis in mammals is controversial. Neogenesis of beta cells after partial ductal ligation has been seen in mice in some studies but not others,[15,19-23] and targeted ablation of beta cells in mice is resolved by proliferation and transdifferentiation.[24-28] Analysis of islets of adult humans with Type I diabetes that died from diabetic ketoacidosis showed that while beta cells continuously apoptosed, there remained beta cells present at death and no markers of proliferation, suggesting some capacity for neogenesis.[29,30] Conversely, zebrafish have an extraordinary capacity to regenerate beta cells by neogenesis after targeted ablation[31,32] and we have identified the progenitor cell that contributes to beta-cell neogenesis in the zebrafish: centroacinar cells (CACs).[33]

CACs are terminal intercalated duct cells – they exist in acini, have long extensions, are connected by tight junctions so they can successfully line pancreatic ducts, and are Notch responsive.[11,33] In addition, they are known to express *sox9b*, a homologue of human *SOX9*, and we have shown that following beta-cell ablation, these *sox9b*-expressing CACs are a source of regenerated beta cells.[34] Humans also have CACs - terminal intercalated duct cells that express *SOX9*[16] and are Notch responsive[35] - but

their role in beta-cell neogenesis is unknown. Given the similarities between these cells in humans and zebrafish, by understanding the mechanisms behind beta-cell neogenesis via CACs in zebrafish, we may be able to exploit these same mechanisms in humans for use in diabetes treatment.

Towards this end, an intriguing target to begin unravelling the mechanisms of beta-cell regeneration is SOX9. The importance of SOX9 in pancreatic identity[36], ductal cell identity[37], and pancreatic progenitor identity[16] has already been established in mammals. Additionally, we recently found that Sox9b helps maintain the progenitor identity of CACs in zebrafish in that heterozygous loss of *sox9b* results in more efficient differentiation of CACs into beta cells after ablation[34]. Given its important role in pancreatic progenitor status across species, we are interested in understanding the transcriptional targets of SOX9 (and Sox9b) to elucidate the genetic program behind pancreatic progenitors and beta-cell neogenesis.

We set out to identify effectors of SOX9 transcriptional activity in human pancreatic cells to reveal molecular mechanisms that drive beta-cell neogenesis using high-throughput sequencing methods. To do so, we utilized a human pancreatic adenocarcinoma line, PANC-1, that represents an undifferentiated, ductal pancreas cell population that can be induced to differentiate toward an endocrine fate.[38] To query the mechanisms of SOX9 regulation in these cells, we integrated RNA-seq and ChIP-seq to identify direct transcriptional targets of SOX9. We found that SOX9 directly regulates *EPCAM*, which encodes a transmembrane protein expressed in stem and progenitor cells in many epithelial tissues[39-42] and is an interesting target of future studies about pancreatic progenitor function.

MATERIALS AND METHODS

RNA-seq library preparation and sequencing

PANC-1 cells were transfected in 24-well plates with either 25 nM of control siRNA (Dharmacon catalog # D-001210-03-05) or 25 nM of *SOX9* siRNA (Dharmacon catalog # M-021507-00-0005) using Lipofectamine 3000 (Thermo). After 48 hours, transfected cells were pooled (4 wells per replicate) and harvested, two replicates from each siRNA condition, and total RNA was isolated using a Qiagen RNeasy kit. RNA-seq libraries were created using the Illumina TruSeq Stranded Total RNA Sample Prep Kit. RNA-seq libraries were pooled and sequenced on the Illumina HiSeq 2000 to a minimum depth of 60 million 2x100 bp reads per library.

RNA-seq alignment, quantification, and analysis

Reads were aligned to hg19 genome with HISAT2 (v2.0.5)[43] and visualized with the Integrative Genomics Viewer.[44,45] Statistical analyses were performed using R (R Core Team, 2017). Gene expression was quantified using the "featureCount" function of the Rsubread package (v1.28.1)[46] to count read overlap with RefSeq genes. Genes with greater than one read across all four samples were submitted to DESeq2 (v1.18.1)[47] to identify genes differentially expressed across conditions (absolute($\log_2$(foldchange)) > 1, adjusted p-value < 0.05). To generate the volcano plot, each gene's $\log_2$(fold change) was plotted against the $-\log_{10}$(adjusted p-value), with genes meeting our criteria for significantly differentially expressed being plotted in red (upregulated) or blue (downregulated). Genes significantly up- and down-regulated were submitted to Enrichr[48,49]. The GO Biological Process was ranked on the basis of the combined score.

Differentially expressed genes were annotated as being directly bound by SOX9 if there was a SOX9 binding event within 1kb (upstream or downstream) of the transcriptional start site (RefSeq, hg19).

ChIP-seq library preparation and sequencing

PANC-1 cells were grown in DMEM supplemented with 10% FBS at 37°C with 5.0% CO_2 and passaged at 70-80% confluency. 2 biological replicates of ChIP-seq were performed essentially as in Lee *et al.*, 2006.[50] Briefly; approximately 2.0 X 10^8 cells were crosslinked in 11% formaldehyde and stopped with 2.5 M glycine before being washed in 1X PBS, lysed, and sonicated for 35 minutes in a Bioruptor at 4°C to achieve a fragment size of approximately 200 bp. An input fraction was set aside and the rest of the lysate was then incubated with 10 ug anti-SOX9 (AB5535, Millipore) overnight at 4°C. Antibody-bound chromatin was then purified using Protein G Dynabeads (Thermo) and crosslinking was reversed overnight at 65°C. ChIP-seq libraries were created using the Illumina TruSeq DNA Sample Prep Kit and quantified using Quant-iT PicoGreen dsDNA assay (Invitrogen). ChIP-seq libraries were pooled and sequenced on the Illumina HiSeq to a minimum depth of 59 million, 1x50bp reads per library.

ChIP-seq alignment, peak calling, and analysis

Reads were aligned to hg19 with Bowtie2 (v2.2.5)[51] in --local mode following TruSeq adapter removal and quality filtering with fastx toolkit (v0.0.14). Following alignment, reads with mapping score < MAPQ30, reads aligning to the mitochondria, and duplicate reads were removed with SAMtools (v1.3.1).[52] ChIP-seq replicates were combined and

peaks were called on this joint file with MACS2 (v2.1.1.20160309)[53] using "callpeak". Peaks with q-value $>10^{-3}$ and those overlapping ENCODE blacklists were removed.[54] These peaks were annotated for their genomic location using CEAS (v1.0.0)[55] of the Cistrome analysis pipeline[56] and the distance of each peak to the nearest gene's transcriptional start site was quantified. The top 1000 most significant SOX9 peaks by q-value were submitted to SeqPos (v1.0.0) under default parameters. The top resulting position weight matrices were matched to motifs in the JASPAR database.[57] These same 1000 peaks were submitted to GREAT (v3.0.0)[58] under default settings except that the association rule was expanded such that "proximal" was defined as 5kb both upstream and downstream. The top 20 GO Biological Process terms by binomial rank were chosen for display and manually grouped by function.

Western blot confirmation of SOX9 knockdown

PANC-1 cells were cultured in 6-well plates and transfected with 100 nM control siRNA (catalogue number above) or 100 nM *SOX9* siRNA (catalogue number above). After 48 hours, cells were washed with PBS, isolated in RIPA buffer with complete, EDTA-free protease inhibitor (Roche) and vortexed. Supernatant was collected after centrifugation. Protein concentration was determined using the Pierce BCA Protein Assay Kit (Thermo Scientific) and 10 ug of protein was run on an Any kD Mini-PROTEAN TGX Precast Protein Gel (Bio-Rad). Transferred at 45V for 90 minutes. Membrane blocked for 1 hour and incubated overnight in primary antibody (Rabbit anti-Sox9 Santa Cruz sc-20095 1:500; N-Cadherin D4R1H XP Rabbit mAb Cell Signaling Technology 13116 1:1000; E-Cadherin 24E10 Rabbit mAb Cell Signaling Technology 3195 1:1000), washed 3 times,

and incubated in anti-rabbit HRP (Cell Signaling 7074S 1:2500) for 1 hour. Developed using SuperSignal West Dura Extended Duration Substrate (Thermo Scientific) and exposed on a ChemiDoc-It^2. Stripped membrane using Restore Western Blot Stripping Buffer (Thermo Scientific) and repeated staining and development as above using rabbit anti-beta-tubulin (Cell Signaling 2128 1:1000) primary.

Antibody staining

PANC-1 cells were grown on gelatin-coated coverslips for 48 hours after siRNA transfection and fixed in 4% paraformaldehyde buffered in 1X PBS. Following 4X5 min washes in 1X PBS, coverslips were blocked in PBST + 10% FBS for 1 hour at room temperature and permeablized in 0.5% Triton in PBS for 20 minutes, incubated with primary antibodies (rabbit anti-SOX9 Santa Cruz sc-20095 1:250; mouse anti-EPCAM Santa Cruz sc-66020 1:100; vimentin D21H3 XP Rabbit mAb Cell Signaling Technology 5741 1:100) at 4°C overnight. Coverslips were washed 4X5 min in blocking, then incubated in secondary antibody (Alexa Fluor 488 donkey anti-rabbit, Alexa Fluor 488 donkey anti-mouse, Cy3 donkey anti-rabbit, Alexa Fluor 647 donkey anti-rabbit, all 1:500, Jackson ImmunoResearch 711-546-152, 715-456-150, 711-166-152, 711-606-152 respectively) at 4°C overnight before 4X5 min final PBST washes and a brief DAPI (1:2500 in PBS) stain. Images were collected using a Nikon A1-si Laser Scanning Confocal microscope.

Q*uantitative PCR confirmation of differentially expressed genes*

PANC-1 cells were cultured in 12-well plates and transfected with 100 nM control siRNA (catalogue number above) or 100 nM *SOX9* siRNA (catalogue number above). After 48 hours, RNA was isolated using Qiagen RNeasy Kit (with DNase digestion step) and cDNA was synthesized using Superscript III (Thermo) with random hexamer primers. 3 biological replicates of the quantitative PCR reactions were run in technical triplicate following the default SYBR green cycling conditions on an Applied Biosystems Viia 7 using 2x Power SYBR Green Master Mix (Applied Biosystems). Expression was calculated using the ΔΔCT method normalized to *GAPDH* expression and control siRNA transfected cells. Primer sequences can be found in **Supplemental Table 2**.[59-61]

Correlation with TCGA pancreatic adenocarcinoma expression patterns

mRNA-sequencing from 178 pancreatic adenocarcinoma samples from the TCGA was accessed and downloaded on March 2, 2018. Read-counts were $\log_2$ normalized after addition of a pseudocount and a heatmap (Raivo Kolde, 2015) was generated for all significantly upregulated and downregulated genes and SOX9's expression patterns in these samples, using hierarchical clustering to group these selected genes into three clusters, and scaling the expression values by column. Individual gene correlation with SOX9 expression was calculated using the Pearson correlation method and for visualization, normalized expression values were plotted.

Phenotypic characterization of epcam mutants

Zebrafish were maintained in system water according to standard methods (Westerfield, 2007). All work involving zebrafish was reviewed and pre-approved by the institutional

care and use committee. CRISPR-generated *epcam* heterozygotes (jh79) were bred with the following previously described lines: *Tg(ela:GFP)*, *Tg(tp1:GFP)*,[62] and *Tg(NeuroD:GFP)*.[63] The resulting offspring were raised to adulthood and genotyped for *epcam* heterozygosity. Fish were in-crossed and embryos were maintained in E3 media (Westerfield, 2007). At 2 dpf the embryos were phenotyped and sorted by small otoliths (*epcam* mutant) and normal otoliths (*epcam* heterozygotes and wildtypes). For examining pancreas morphology, at 4 days dpf the larvae were fixed in 4% paraformaldehyde (PFA) for 48 hours at 4 °C and then imaged in methylcellulose on a Nikon AZ100 microscope. For examining CAC morphology, the midbodies of the larvae (heads digested for genotyping to confirm otolith phenotype) were fixed at 5 dpf in 4% PFA for at least 24 hours at 4 °C. The gut with the pancreas attached was dissected out of each of the fixed larvae. These dissected samples were dehydrated, rehydrated, blocked, stained, mounted, and imaged as per Part II (rabbit anti-GFP Invitrogen A11122 1:400; Alexa Fluor 488 donkey anti-rabbit Jackson ImmunoResearch 711-546-152 1:200). CACs were counted from these images using ImageJ. For examining CAC differentiation, larvae were treated from 3 to 5 dpf in either 0.5% DMSO (diluted from 100% stock) or 0.625 uM RO4929097 (Selleckchem S1575, diluted from 10 mM stock in DMSO) in E3. Midbodies of larvae were fixed at 5 dpf (heads digested to confirm genotype of otolith phenotype) and dissected, stained, and imaged as above. Secondary islets counted using ImageJ.

RESULTS

SOX9 modulates the transcription of proliferation and cilia genes in PANC-1 cells

We took a two-step approach to identify direct transcriptional targets of SOX9 in PANC-1 cells; namely, RNA-seq following *SOX9* knockdown and then ChIP-seq to identify SOX9 binding sites. To identify transcripts that are regulated by SOX9 activity, we performed RNA-seq in PANC-1 cells that had been transfected with either a *SOX9* siRNA or a control siRNA. Following *SOX9* siRNA transfection, *SOX9* knockdown was confirmed using both Western blotting (**Figure 1A**) and immunofluorescence of fixed cells (**Figure 1B**). To identify genes regulated by SOX9, we sequenced total RNA extracted from PANC-1 cells transfected with either control or *SOX9* siRNA and identified genes that are differentially expressed between knockdown conditions. We identified 93 differentially expressed genes with 60 genes upregulated and 33 downregulated (**Figure 1C; Table 1**).

To confirm the identity of the top differentially expressed genes, we performed qRT-PCR in siRNA-treated PANC-1 cells for the top five up- and down-regulated genes. In doing so, we confirmed the differential expression of these ten genes, except the downregulated gene *SKIV2L* (**Figure 1D**). While *SKIV2L* demonstrated the largest fold change of the downregulated genes, it was also nearest the acceptable p-value cut-off and thus may be a false positive.

In order to further validate the differential gene expression results, we analyzed publicly available RNA-seq data from 178 pancreatic adenocarcinoma samples in The Cancer Genome Atlas. In these samples, *SOX9* is highly expressed and as such, we expected to observe directions of effect opposite to those observed in our induced knockdown experiments. We clustered our differentially expressed genes based on their expression patterns in the tumor samples and observe that in general, corroborating our

knockdown studies, upregulated genes clustered together and were lowly expressed in the tumor samples, and downregulated genes clustered together and with *SOX9* and are highly expressed (**Figure 2A**). Furthermore, at an individual gene level, we correlated *SOX9* expression with each differentially expressed gene to examine how closely the genes are co-regulated in these tumor samples and observed there to be a high degree of correlation between the differentially expressed genes and *SOX9* expression (**Supplementary Table 1**). For example, the upregulated gene with the strongest degree of negative correlation with *SOX9* expression is *CCDC13* (r = -0.50), bolstering our observation that SOX9 negatively regulates this gene (**Figure 2B**). Conversely, expression of the downregulated gene, *ESRP1*, is strongly positively correlated with *SOX9* expression (r = 0.67), further suggesting that SOX9 positively regulates this gene's expression (**Figure 2C**). Overall, these data serve to validate observations from our genome wide RNA-seq analyses and provide additional support for our observed transcriptional targets of SOX9.

Finally, to assess the biological consequences of these differentially expressed genes, we explored their individual functions and gene ontology (GO) terms. Genes that are down-regulated following *SOX9* knockdown include genes with established roles in cancer motility (*ESRP1*[59]), cell-cell adhesion (*TINAGL1*[64,65]), obesity and insulin resistance (*RGCC*[66]), and cancer stem cell maintenance (*EPCAM*[67]). Down-regulated genes were collectively enriched for biological processes associated with Notch signaling and the negative regulation of proliferation (**Figure 1E**), suggesting a role for SOX9 in negatively regulating proliferation.

As a whole, upregulated genes were enriched for processes associated with cilia development, assembly, and movement (**Figure 1F**), suggesting that SOX9 typically suppresses these processes. Interestingly, the most highly upregulated genes following *SOX9* knockdown are *LRRC6* and *SPEF1*, which have known roles in regulating primary cilia, important features of ductal epithelial cells.[68-70] In all, these observations may indicate that SOX9 serves to restrict the differentiation of pancreas progenitor cells toward an epithelial fate by promoting the expression of genes important for maintaining a progenitor status.

SOX9 binding occurs primarily at transcription start sites and regulates pancreatic functions

We next set out to identify putative SOX9-responsive regulatory regions, undertaking anti-SOX9 ChIP-seq. Following pull-down, sequencing, and alignment, our analysis identified 47,858 SOX9 binding sites in PANC-1 cells. We then analyzed the sequence underlying the top 1000 most significant SOX9 binding events to identify transcription factor motifs present at these sites. The top enriched motif was a "tail-to-tail" palindrome with high similarity to the SOX9 consensus motif (**Figure 3A**). This result supports previous observations in chondrocytes that SOX9 can function as a homodimer.[71] The second highest enriched motif matched the binding sequence for FOS::JUN (**Figure 3B**) which has been previously reported to bind in conjunction with SOX9 in chondrocytes.[72] Similar to findings from other groups[73,74], we observe an enrichment of SOX9 binding events at gene promoters (8.8% of SOX9 peaks; **Figure**

3C), with diminishing proportions of SOX9 binding events occurring as the distance to the transcriptional start site increases (**Figure 3D**).

Next, we sought to interrogate the potential functional outcome of SOX9 binding in PANC-1 cells. We performed functional annotation of the genes proximal to SOX9 binding sites and found many GO biological processes that match with SOX9's known roles (**Figure 3E**). These include: 1) endocrine pancreas development, reflecting the known function of SOX9 activity in the pancreas; 2) stem cell maintenance, reflecting the participation of SOX9 in maintaining pancreatic progenitor identity[34] and; 3) ossification and osteoblast differentiation, which reflects known functions of SOX9 in bone development.[75,76] Taken collectively, these data suggest that SOX9 acts in PANC-1 cells to regulate target genes important to pancreas biology, in a manner consistent with previously reported modes of action in chondrocytes.

Direct targets of SOX9 overlap with known pancreatic ductal genes

To narrow down the list of differentially expressed genes to those most biologically relevant, we combined three datasets: 1) SOX9 binding events from our ChIP-seq experiment to identify direct binding targets of SOX9; 2) genes with enriched expression in ductal cells (versus acinar or endocrine cells) of the adult zebrafish pancreas[18] and; 3) genes enriched in zebrafish CACs which can be used as CAC markers.[33] By combining these three data sets we sought to find genes that were not only direct targets of SOX9 – i.e. those that were differentially expressed following *SOX9* knockdown and had a SOX9 binding site proximal to their promoter – but also relevant to

the biology of the zebrafish pancreatic ductal cells, and specifically CACs, not just the molecular underpinnings of human PANC-1 cells.

We observed that the majority of genes upregulated with *SOX9* knockdown are not direct targets of SOX9 (57% of all upregulated genes and 70% of the top ten are not bound by SOX9), while all but one of the top ten genes downregulated with *SOX9* knockdown are direct targets (**Table 2**), and 64% of downregulated genes overall are bound. Several downregulated genes have enriched expression in pancreatic ductal cells while the only upregulated gene with ductal expression is *LRRC6*. Finally, *EPCAM* appears to be a promising candidate gene for further investigation because it is a direct target of SOX9, has enriched expression in zebrafish ductal cells, and is a marker of CACs (**Table 2**).

SOX9 directly regulates expression of EPCAM

Given its promising expression in zebrafish pancreatic ductal cells, specifically CACs, we examined the relationship between SOX9 and *EPCAM*. *EPCAM* is a gene encoding a transmembrane protein that is a well-known marker of epithelium and has roles in the regulation of pancreas progenitor differentiation and cell adhesion.[39,67] Traces from our RNA-seq and ChIP-seq display the decreased expression of *EPCAM* with SOX9 knockdown and a large SOX9 binding peak centered on the *EPCAM* transcriptional start site and promoter (**Figure 4A**). Additionally, we performed EPCAM and SOX9 antibody staining in PANC-1 cells transfected with either control or *SOX9* siRNA. In control-transfected cells, SOX9 was expressed in all cell nuclei and EPCAM was expressed at the plasma membrane in all cells, albeit with varying intensity. Following *SOX9* knockdown,

SOX9 expression was reduced or absent in nuclei, and EPCAM expression was reduced or absent (**Figure 4B**). These results support the conclusion that SOX9 directly regulates *EPCAM* expression in PANC-1 cells.

Furthermore, as a preliminary validation of the relevance of this relationship *in vivo*, we examined the co-regulation of *SOX9* and *EPCAM* in the TCGA pancreatic adenocarcinoma samples, as above. In doing so, we observe a strong positive correlation of *SOX9* and *EPCAM* expression (r = 0.58; **Figure 4C**), suggesting that *in vivo*, as well as *in vitro*, SOX9 is a positive regulator of *EPCAM* expression.

Epcam does not appear to be necessary for normal CAC function

Because it is a direct target of SOX9 in PANC-1 cells and a CAC marker in the adult zebrafish, we wanted to pursue the role of Epcam in the biology of CACs. To do this, we used a CRISPR-generated knockout of *epcam* where there is a 12 base-pair deletion at the splice acceptor site of exon 4 (**Figure 5A**). We were able to phenotype *epcam* mutants by screening for small otoliths at 2 dpf (data not shown), a phenotype that has been previously shown in a different *epcam* knockout model.[77] We first looked at the gross morphology of the pancreas using the *Tg(ela:GFP)* line that marks all acinar cells of the pancreas. At 4 dpf there appeared to be no difference in size or morphology of the pancreas between larvae with small otoliths (representing *epcam* mutants) and normal otoliths (representing *epcam* heterozygotes and wildtypes) (**Figure 5B**). Since our previous RNA-seq work showed that *epcam* is specifically a marker of CACs in the zebrafish[33] we wanted to next look at the morphology and function of CACs in larval *epcam* mutants. We used the *Tg(tp1:GFP)* line to mark CACs and assessed the number

and morphology of these cells. At 5 dpf, both the *epcam* mutants (screened by small otoliths) and the heterozygotes and wildtypes (screened by normal otoliths) had CACs with normal morphology – notice how the cells wrap around the head and down the tail of the pancreas, each with long extensions (**Figure 5C**). When these cells are counted across samples, the *epcam* mutants have the same number of CACs as their non-mutant siblings (**Figure 5D**). Finally, we wanted to assess the function of CACs in *epcam* mutants by looking at their ability to differentiate into secondary islets. We have shown previously that treatment with the Notch inhibitor RO4929097 causes early development of secondary islets from CACs.[78] Treatment of both *epcam* mutants and their non-mutant siblings (crossed with a *Tg(NeuroD:GFP)* line) from 3 to 5 dpf with either RO4929097 or a DMSO control revealed that all *epcam* genotypes are able to increase their number of secondary islets at 5 dpf with RO4929097 treatment versus DMSO. (**Figure 5E**). Taken together, these data suggest that while *epcam* is a direct target of SOX9 and a marker of CACs, it does not appear to be necessary for the normal biology and function of CACs.

DISCUSSION

We previously demonstrated that Sox9b functions downstream of both Notch signaling and Retinoic Acid signaling in CACs.[34] All of these pathways are responsible for maintaining the progenitor identity of CACs. Because understanding the balance between progenitor maintenance and endocrine differentiation is central to characterizing beta-cell neogenesis, we sought to further elucidate the differentiation process by finding the downstream targets of Sox9b to better understand how it functions as a central transcription factor in CAC progenitor identity.

By performing RNA-seq and ChIP-seq on PANC-1 cells we were able to identify both direct targets (change in expression with SOX9 knockdown and SOX9 binding peak near promoter) and indirect targets (change in expression with SOX9 knockdown but no SOX9 binding peak) of SOX9. Because a number of the direct targets – like EpCAM and ESRP1 – are associated with epithelial cells, we wondered if a decrease in these genes results in an epithelial-to-mesenchymal transition (EMT) and this change in cell state alters the overall transcriptional profile of the PANC-1 cells. But simple EMT induction does not explain the changes in transcription we saw - looking at EMT markers by Western, IF, and qPCR showed that not only was there no EMT, but PANC-1 cells are already mesenchymal in nature before SOX9 knockdown (**Supplementary Figure 2**). So a change to a more mesenchymal phenotype is not responsible for the transcriptional differences seen in SOX9 knockdown. Because Sox9b is known to help CACs maintain their progenitor identity,[34] it's possible that knockdown of SOX9 in PANC-1 cells induces differentiation. This idea fits with our RNA-seq results – knockdown of SOX9 caused an increase in the expression of many ciliary genes which is a known consequence of differentiation.[79]

GO analysis of genes downregulated with SOX9 knockdown showed that SOX9 is important for the positive regulation of Notch receptor targets. This aligns well with previous research, as the role of SOX9 in mediating the expression of downstream Notch signaling targets is well-established.[80-83] Understanding this intricate cross-talk between SOX9 and Notch will be important to being able to manipulate progenitor differentiation to endocrine cells.[34,78]

In comparison to previous work in other cell systems, we were able to easily see the SOX9 binding consensus sequence by pulling out the most enriched sequence at binding peaks - unlike the results of ChIP-seq performed in hair follicle stem cells.[84] They found that SOX9 was promiscuous in the sequences it bound to and never saw the consensus sequence. In addition, we saw that SOX9 preferentially bound to promoters, no matter the target gene, unlike what was seen in developing chondrocytes where SOX9 bound promoters for normal cellular functions and enhancers for chondrocyte-specific transcription.[85] These differences suggest that SOX9 may vary in how it acts as a transcription factor between different cell types.

The direct targets of SOX9 that we found have some interesting connotations for both the ductal nature of CACs and their progenitor role. TINAGL1 is a matricellular protein that is known to bind integrins and laminins and is involved in both post-implantation development in the uterus[65,86] and vascular smooth muscle adhesion.[64,87,88] It's homolog TINAG is important in tubulogenesis in the kidney.[89] CACs are known to line the branching ducts of the pancreas, so an extracellular molecule important for cell-adhesion (and the cell-cell signaling that goes along with it) makes biological sense for having an important SOX9-mediated role. ESRP1 is a regulator of splicing and is known for predicting favorable outcomes in cancer - i.e. its expression (and therefore splicing patterns of things like *FGFR2*) is thought to suppress cancer cell motility and therefore metastasis.[59,90-92] This would make biological sense in the context of CACs and regeneration - expression of Sox9b and therefore ESRP1 could promote the epithelial nature of CACs while loss of these proteins would promote a more migratory, mesenchymal nature which is necessary for CACs to move to ablated islets and become

endocrine cells. All of these genes would be interesting targets to follow up on by examining their expression in the zebrafish pancreas, developing knockouts, and assessing their importance in CAC maintenance and biology.

Finally, we showed that SOX9 regulates the expression of EpCAM, a gene that encodes a single-pass transmembrane glycoprotein that localizes to tight junctions.[39] In addition to its role in cell adhesion, EpCAM can also undergo proteolytic cleavage to produce intra- and extracellular fragments that participate in signaling and transcriptional activation.[67] Although EpCAM is expressed broadly in epithelial tissues, higher expression is found in cells that are actively undergoing proliferation and differentiation events. Thus, EpCAM serves as a marker of stem and progenitor cell populations in the intestine, liver, and salivary gland.[40-42] It is also expressed in human and murine embryonic stem cells, where it may function upstream of the well-known pluripotency factors OCT4 and SOX2.[93,94] In the human fetal pancreas, EpCAM expression is enhanced in progenitor cells that are budding from the ductal epithelium to form new endocrine cells.[39] In the adult pancreas, it is most highly expressed in intercalated ducts,[39] which closely resemble CACs and have been proposed to serve as an endocrine progenitor population during regeneration.[11] Intriguingly, transgenic overexpression of EpCAM in the mouse pancreas provokes the development of large endocrine islets.[95] Within the developing zebrafish liver EpCAM is expressed in Notch responsive progenitor cells called Biliary Epithelial Cells (BECs) that act as progenitors for hepatocytes during liver damage and development.[96,97] Many parallels can be drawn between BECs and the CACs of the pancreas. These cell types both line ducts, and Notch signaling as well as Sox9 play an important role in maintaining the progenitor status of

both. Although it seems disheartening that our CRISPR-generated *epcam* knockout zebrafish line does not show an obvious deficit in CAC function, this actually matches the phenotype of *sox9b* heterozygotes. These fish did not have an obvious pancreatic or CAC phenotype and therefore we did not see the important role that *sox9b* played in CAC biology until we looked at ablation and regeneration.[34] The logical next step in this work then is to see whether *epcam* mutants regenerate faster or slower than their non-mutant siblings after ablation of beta cells. This will tell us whether *epcam* is downstream of *sox9b* in its role maintaining CAC identity or whether *epcam* instead is downstream of *sox9b* in a different biological context. Because EpCAM is expressed in the mammalian pancreas and in the CACs of zebrafish, understanding how EpCAM acts downstream of Sox9 in the maintenance and identity of endocrine progenitor cells will help us better define the mechanisms behind endogenous increases in beta-cell mass.

Figure 1. Knockdown of SOX9 results in an increase of ciliary gene expression and a decrease in expression of genes negatively regulating proliferation. (A) Western blot and (B) immunofluorescence confirms knockdown of SOX9 protein following *SOX9* siRNA treatment. Scale bar is 100 um. (C) A volcano plot of adjusted p-value versus fold change upon SOX9 knockdown indicates that 93 genes exhibit significantly altered expression (33 decreased and 60 increased). (D) Quantitative PCR confirms all but one (*SKIV2L*) of the top five upregulated and top five downregulated genes observed with RNA-seq. 3 biological replicates per gene, error bars represent standard deviation (E) GO analysis of downregulated genes reveals a role for SOX9 in Notch signaling as well as in the regulation of proliferation. (F) GO analysis of upregulated genes is enriched for ciliary development and function. Neg, Negative; Pos, Positive; reg, regulation.

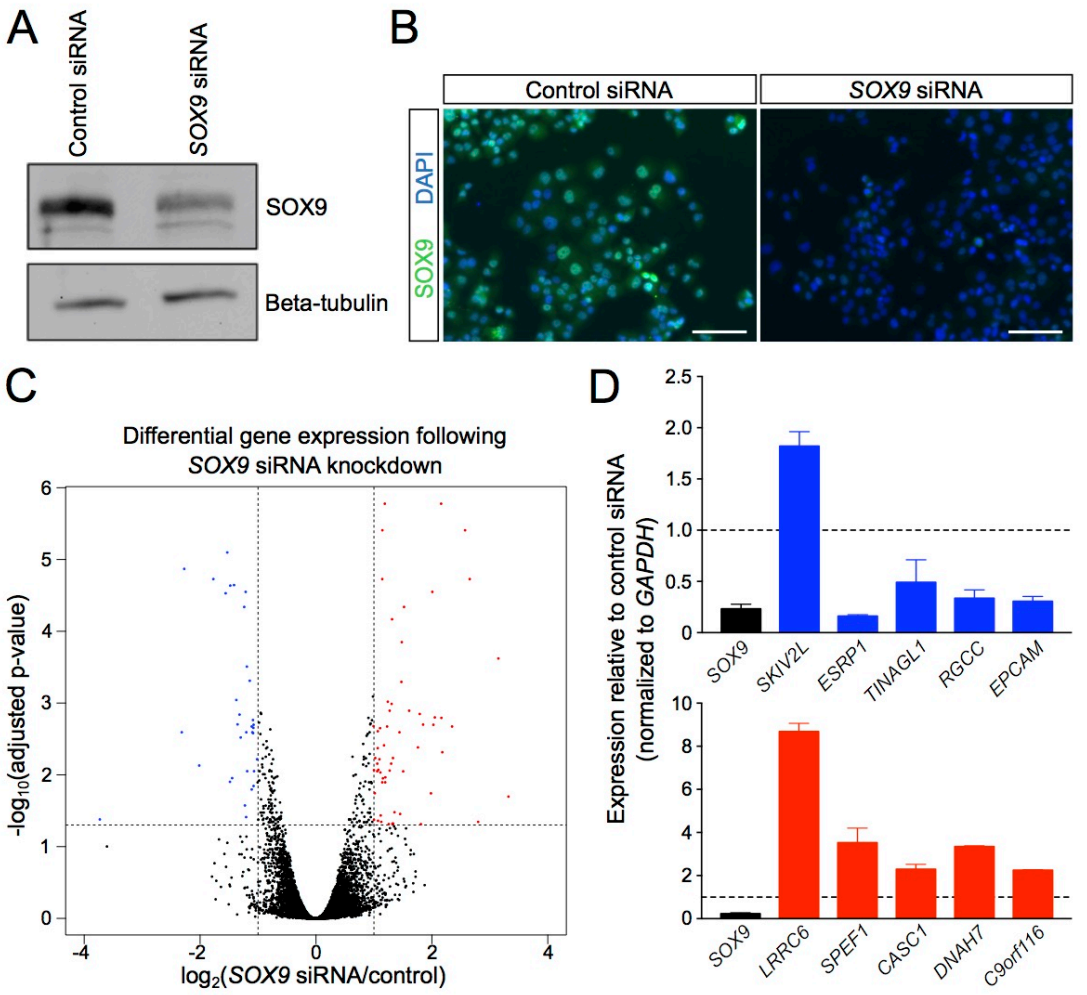
A
Control siRNA
SOX9 siRNA
SOX9
Beta-tubulin
B
Control siRNA
SOX9 siRNA
DAPI
SOX9
C
Differential gene expression following
SOX9 siRNA knockdown
-log10(adjusted p-value)
log2(SOX9 siRNA/control)
D
Expression relative to control siRNA
(normalized to GAPDH)
SOX9
SKIV2L
ESRP1
TINAGL1
RGCC
EPCAM
SOX9
LRRC6
SPEF1
CASC1
DNAH7
C9orf116
E
Downregulated
GO Biological Process - Combined Score
Pos. reg. of transcription of Notch receptor target
Neg. reg. of cell proliferation involved in kidney development
Neg. reg. of cell proliferation in bone marrow
Neg. reg. of fibroblast proliferation
Neg. reg. of cell proliferation involved in compound eye morphogenesis
Neg. reg. of hemocyte proliferation
Neg. reg. of cell proliferation involved in heart morphogenesis
Neg. reg. of fat cell proliferation
Neg. reg. of myoblast proliferation
Neg. reg. of germ cell proliferation
F
Upregulated
GO Biological Process - Combined Score
Motile cilium assembly
Inner dynein arm assembly
Outer dynein arm assembly
Non-motile cilium assembly
Axoneme assembly
Ciliary basal body-plasma membrane docking
Epithelial cilium movement
Cilium movement involved in cell motility
Ciliary transition zone assembly
Cytosolic ciliogenesis

Figure 2. Expression data from pancreatic adenocarcinoma samples corroborate the expression patterns seen in PANC-1 cells. (A) Expression analysis of the TCGA pancreatic adenocarcinoma sample data set indicate that upregulated genes identified by RNA-seq in PANC-1 cells tend to cluster together and are lowly expressed in these samples. Further, downregulated genes identified by RNA-seq in PANC-1 cells tend to cluster together and with *SOX9* and are highly expressed. (B) At an individual gene level, *CCDC13*, a gene that is upregulated following *SOX9* knockdown, is negatively correlated with *SOX9* expression, suggesting that SOX9 negatively regulates this gene. (C) Conversely, *ESRP1*, a gene that is downregulated following SOX9 knockdown, is positively correlated with SOX9 expression, suggesting that SOX9 positively regulates this gene.

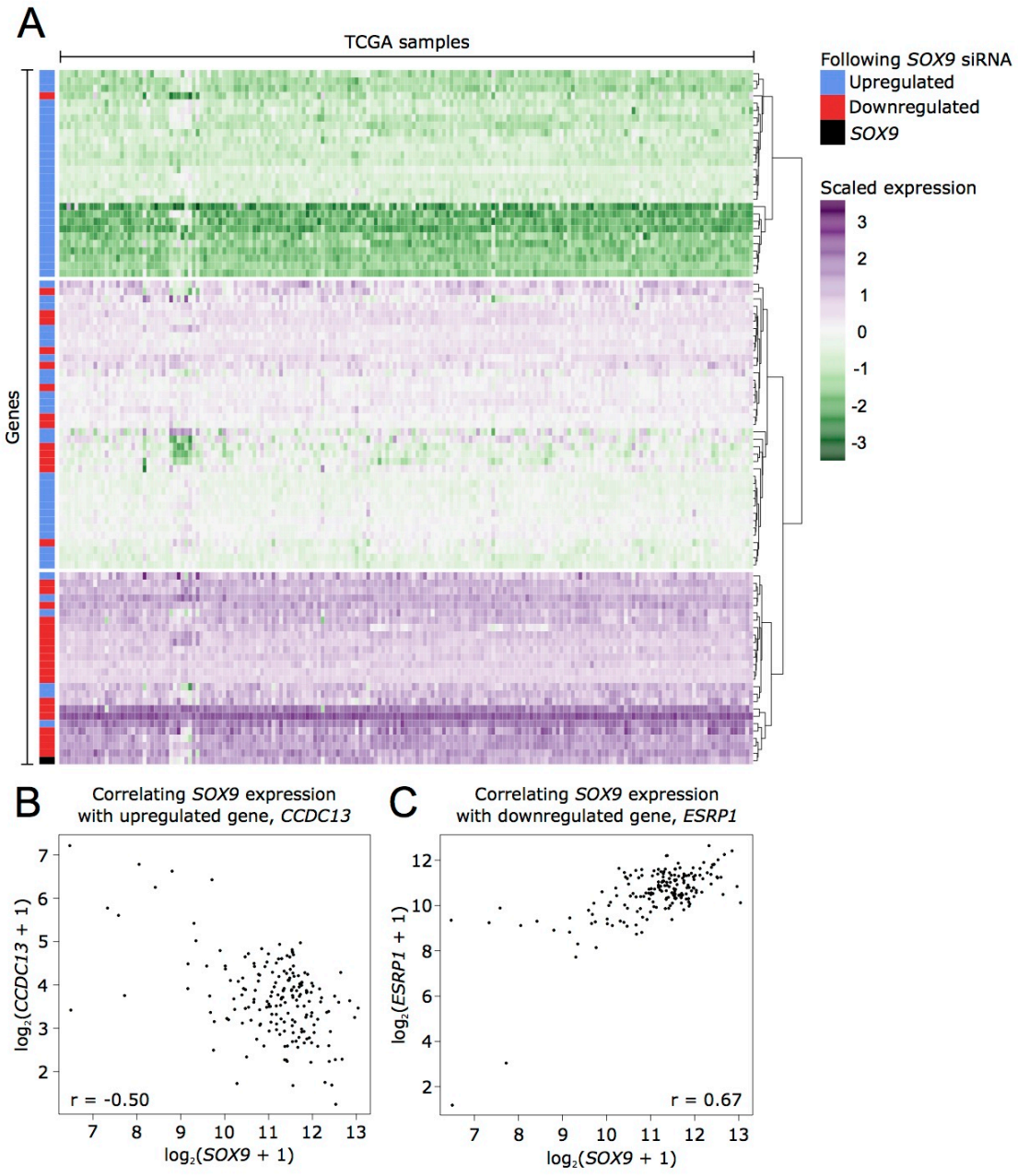
A
TCGA samples
Genes
Following SOX9 siRNA
Upregulated
Downregulated
SOX9
Scaled expression
3
2
1
0
-1
-2
-3
B
Correlating SOX9 expression with upregulated gene, CCDC13
log2(CCDC13 + 1)
log2(SOX9 + 1)
r = -0.50
C
Correlating SOX9 expression with downregulated gene, ESRP1
log2(ESRP1 + 1)
log2(SOX9 + 1)
r = 0.67

Figure 3. Characteristics of SOX9 gene regulation include promoter proximal binding and regulation of genes important to pancreatic biology. (A) The most common motif seen at SOX9 binding sites is a homodimer of the forward and reverse known SOX9 binding sequences (tail to tail). (B) The second most common motif at SOX9 binding sites is recognized by FOS::JUN. (C) SOX9 binding is enriched at promoters (≤1000 base-pairs upstream of a transcription start site). (D) As distance from the transcriptional start site increases, the proportion of SOX9 binding events decreases. (E) The nearest genes to SOX9 binding sites are enriched for GO terms related to known SOX9 biology, including endocrine pancreas functions.

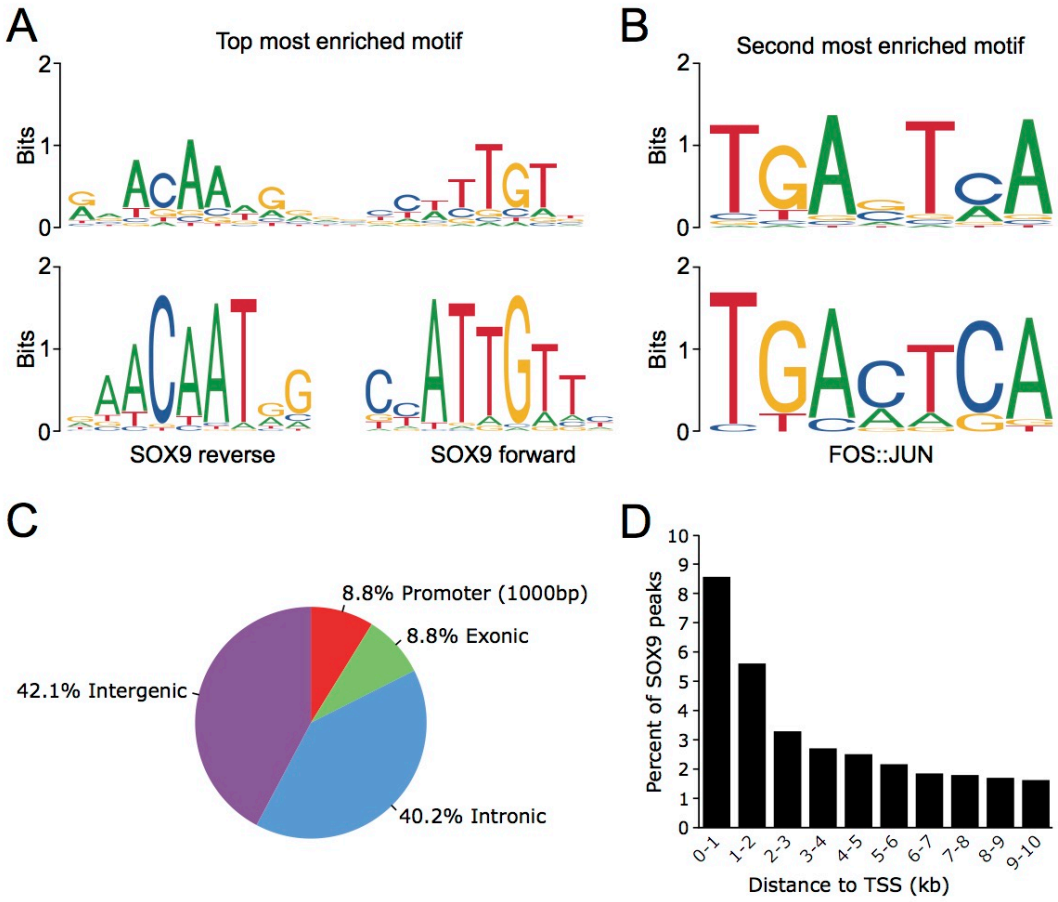
A
Top most enriched motif
Bits
SOX9 reverse
SOX9 forward
B
Second most enriched motif
FOS::JUN
C
8.8% Promoter (1000bp)
8.8% Exonic
42.1% Intergenic
40.2% Intronic
D
Percent of SOX9 peaks
Distance to TSS (kb)
0-1
1-2
2-3
3-4
4-5
5-6
6-7
7-8
8-9
9-10
E
Binomial Fold Enrichment
Endocrine pancreas development 2.82
Pancreas development 2.23
Somatic stem cell maintenance 3.19
Stem cell maintenance 2.19
Osteoblast differentiation 2.44
Ossification 2.20
Prostate gland morphogenetic growth 6.95
Prostate gland growth 4.23
Male sex determination 4.06
Embryonic placenta morphogenesis 4.76
Labyrinthine layer development 3.94
Embryonic placenta development 2.80
Placenta development 2.77
Endocardial cushion morphogenesis 3.91
Heart valve morphogenesis 3.72
Lactation 3.74
Mammary gland development 2.07
Reactive oxygen species metabolic process 3.28
Secretion by tissue 3.18
Body fluid secretion 3.01

Figure 4. RNA-seq and ChIP-seq in combination reveal *EPCAM* to be a direct target of SOX9. (A) Traces corresponding to RNA-seq and ChIP-seq reads near the *EPCAM* gene confirm *SOX9* knockdown and reveal SOX9 binding at the *EPCAM* transcription start site. (B) Immunofluorescence staining of PANC-1 cells confirms knockdown of both SOX9 and EPCAM protein by si*SOX9*. Scale bar is 100 um. (C) Expression of *EPCAM* and *SOX9* in TCGA pancreatic adenocarcinoma samples are positively correlated, suggesting that *EPCAM* expression is upregulated by SOX9.

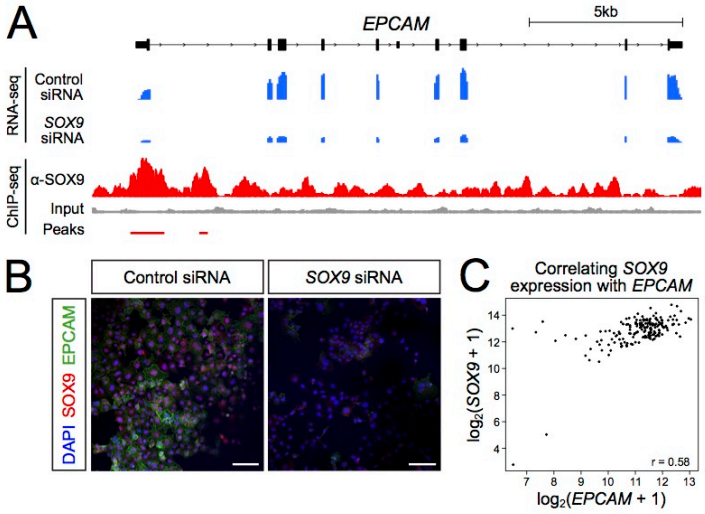
A
EPCAM
5kb
RNA-seq
Control siRNA
SOX9 siRNA
ChIP-seq
α-SOX9
Input
Peaks
B
Control siRNA
SOX9 siRNA
DAPI SOX9 EPCAM
C
Correlating SOX9 expression with EPCAM
log2(SOX9 + 1)
log2(EPCAM + 1)
r = 0.58

Figure 5. *Epcam* mutants show no obvious abnormalities in terms of centroacinar cell structure and function. (A) CRISPR-generated mutant allele removes splice site at the start of exon 4 of *epcam*. Top sequence is wildtype and bottom sequence is CRISPR-generated mutant. End of intron in lower case, beginning of exon 4 in upper case, splice acceptor site highlighted in green. (B) A *Tg(ela:GFP)* background in larval zebrafish at 5 dpf shows very little difference in pancreas size between *epcam* wildtypes/heterozygotes and mutants. (C,D) A *Tg(tp1:GFP)* background reveals no difference in the morphology or number of CACs between *epcam* wildtype/heterozygote and mutant zebrafish at 5 dpf. (E) CACs in *epcam* mutant zebrafish are still able to differentiate effectively with inductive drug treatment (treatment with either DMSO or RO4929097). Normal otoliths (NO), small otoliths (SO).

A

gctttcaccccatagTGGTTCCCAAGTGCTTCCTCATGCAA

gctttcac . . . . . .CCCAAGTGCTTCCTCATGCAA

B

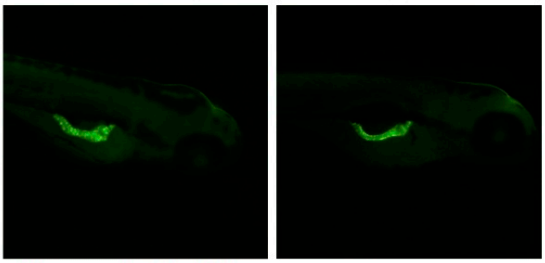

Normal Otoliths Small Otoliths

C

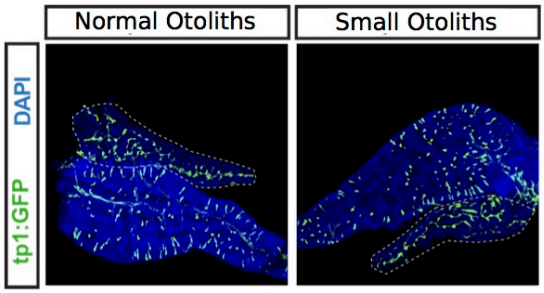

D

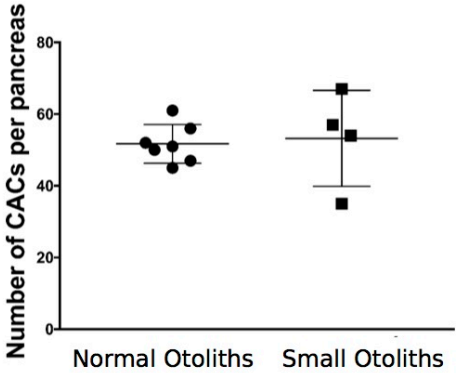

E

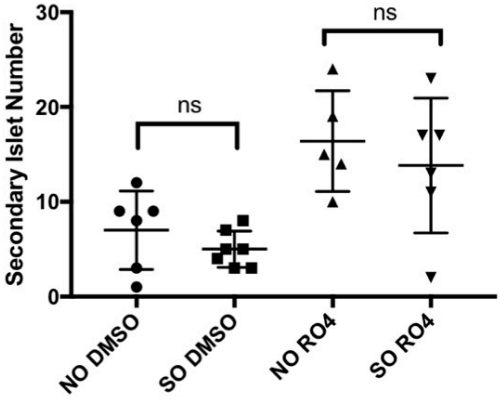

Supplementary Figure 1. Changes in gene expression from SOX9 knockdown do not correspond with changes in cell state. (A) Immunofluorescence for the mesenchymal marker vimentin is present uniformly in PANC-1 cells. (B) There is no change in N-cadherin or E-cadherin expression by Western blot between PANC-1 cells treated with siControl versus siSOX9. (C) Quantitative PCR shows that while there is a general decrease in expression of *FGFR2* with SOX9 knockdown, there is no change in the ratio between its splice isoforms or the splice isoforms of *FGFR3*, indicative of no EMT.[60,61] 3 biological replicates per gene, error bars represent standard deviation.

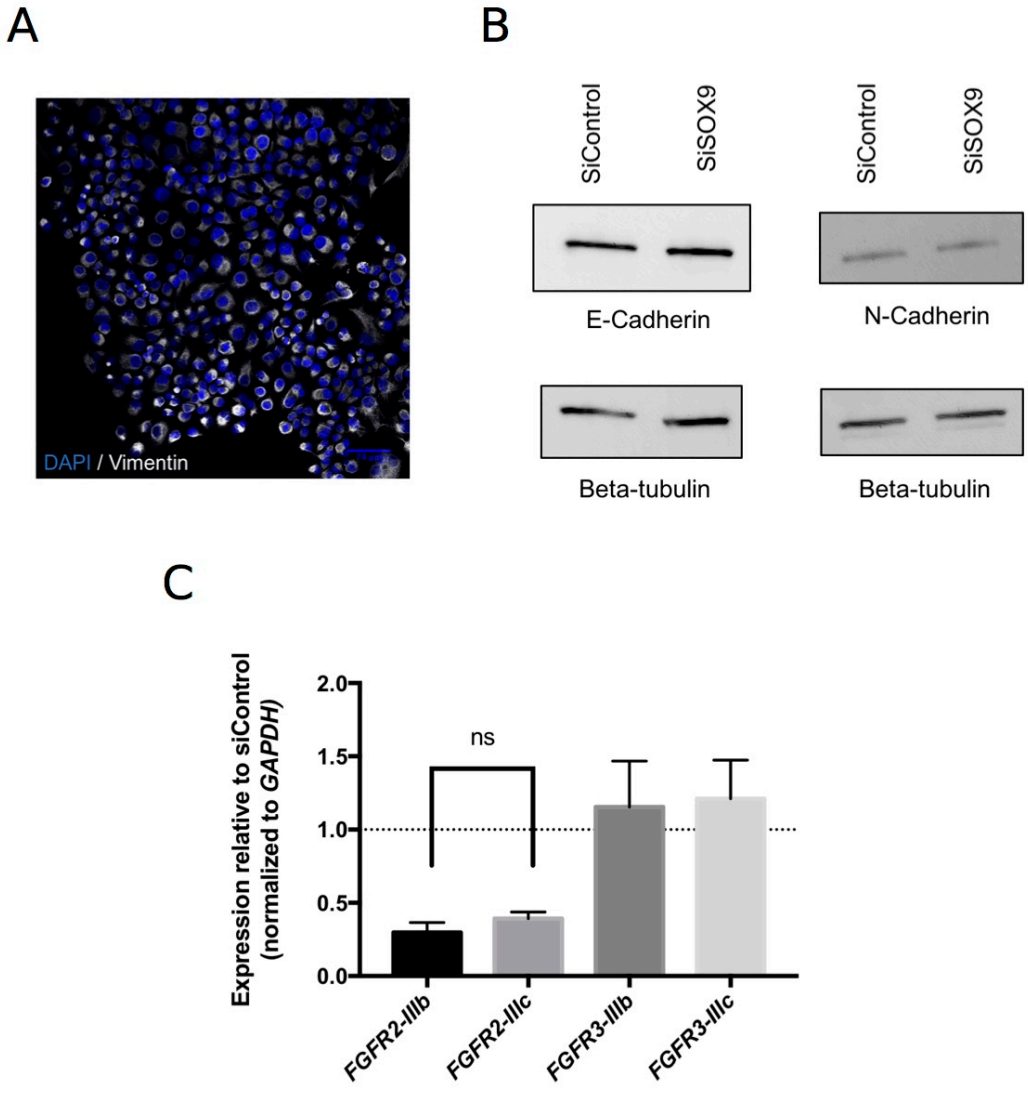
A
DAPI / Vimentin
B
SiControl
SiSOX9
SiControl
SiSOX9
E-Cadherin
N-Cadherin
Beta-tubulin
Beta-tubulin
C
Expression relative to siControl
(normalized to GAPDH)
2.0
1.5
1.0
0.5
0.0
ns
FGFR2-IIIb
FGFR2-IIIc
FGFR3-IIIb
FGFR3-IIIc

Table 1 Top ten upregulated and downregulated genes following *SOX9* siRNA knockdown

	Gene	$\log_2$ (*SOX9* siRNA/control)	p-value (adjusted)
Upregulated	*LRRC6*	3.332	1.98E-02
	SPEF1	3.158	2.36E-04
	CASC1	2.809	4.45E-02
	DNAH7	2.663	1.85E-05
	C9orf116	2.583	3.86E-06
	CFAP69	2.358	2.09E-03
	CCDC13	2.191	4.77E-03
	AXIN2	2.175	1.59E-03
	C6orf165	2.169	1.64E-06
	ROPN1L	2.061	1.56E-03
Downregulated	*TUB*	-1.437	1.09E-02
	LIN7C	-1.470	2.28E-05
	SLC45A3	-1.475	1.23E-02
	DDAH1	-1.522	7.86E-06
	CENPM	-1.550	2.91E-05
	EPCAM	-1.762	1.85E-05
	RGCC	-2.006	7.30E-03
	TINAGL1	-2.264	1.33E-05
	ESRP1	-2.307	2.52E-03
	SKIV2L	-3.721	4.11E-02

Table 2 Assessing the top differentially expressed genes for evidence of direct SOX9 regulation, expression in pancreatic ductal cells, and ability to mark CACs

	Gene	Direct target of SOX9?	Enriched ductal expression?	CAC marker?
Upregulated	*LRRC6*	Yes	Yes	No
	SPEF1	Yes	No	No
	CASC1	No	No	No
	DNAH7	No	No	No
	C9orf116	No	No	No
	CFAP69	Yes	No	No
	CCDC13	No	No	No
	AXIN2	No	No	No
	C6orf165	No	No	No
	ROPN1L	No	No	No
Downregulated	*TUB*	Yes	No	No
	LIN7C	Yes	No	No
	SLC45A3	Yes	No	No
	DDAH1	Yes	No	No
	CENPM	Yes	No	No
	EPCAM	Yes	Yes	Yes
	RGCC	No	Yes	No
	TINAGL1	Yes	Yes	No
	ESRP1	Yes	Yes	No
	SKIV2L	Yes	No	No

Supplementary Table 1 Correlation of *SOX9* expression with the top ten up- and down-regulated genes

	Gene	Pearson correlation
Upregulated	*LRRC6*	0.21
	SPEF1	-0.13
	CASC1	-0.14
	DNAH7	-0.02
	C9orf116	0.07
	CFAP69	-0.22
	CCDC13	-0.50
	AXIN2	-0.17
	C6orf165	-0.31
	ROPN1L	-0.35
Downregulated	*TUB*	-0.56
	LIN7C	0.04
	SLC45A3	0.48
	DDAH1	0.35
	CENPM	0.24
	EPCAM	0.58
	RGCC	-0.30
	TINAGL1	0.57
	ESRP1	0.67
	SKIV2L	0.03

Supplementary Table 2 List of primers used for qPCR

Gene	F primer	R primer	Reference
GAPDH	GCACCGTCAAGGCTGAGAAC	ATGGTGGTGAAGACGCCAGT	Ishii et al. 2014
SOX9	GGGCACCGGCCTCTACTCCA	TCCCAGTGCTGGGGGCTGT	
LRRC6	CGCCATGGGCTGGATCACAGAA	ATGCAACGAGAGTTCCTCCAGGG	
SPEF1	AGCGATGGAGTCCTTGTTGCAGAG	TGGAGAGAGTTGGCGGGGACA	
CASC1	AGGTGTTTTCCTGAAGCAGAGA	AGGATCAGGACTCCCATCACA	
DNAH7	TGCCTCTATCGTCCTAGGGG	GCTGGCCGATTTATCCTGCT	
C9orf116	GGAGAGGACCAGCGACTACT	ACAGCCTTCTGGGTCCTGTA	
SKIV2L	CGGGAGCGAATGCAGATACA	GTTCGGAGCACCTCTACTCG	
ESRP1	CAATATTGCCAAGGGAGGTG	GTCCCCATGTGATGTTTGTG	Ishii et al. 2014
TINAGL1	TCCCAAACAGCAGTTGGATGTA	GGTTCTTGGTCACACTGCCA	
RGCC	GCACCTGGAGCGCATGAAGC	TGAATCTGCACTCTCCGAGTCGCT	
EPCAM	CGCGTTCGGGCTTCTGCTTG	ATTTGGCAGCCAGCTTTGAGCA	
FGFR2-IIIb	CGTGGAAAAGAACGGCAGTAAATA	GAACTATTTATCCCCGAGTGCTTG	Ranieri et al. 2015
FGFR2-IIIc	TGAGGACGCTGGGGAATATACG	TAGTCTGGGGAAGCTGTAATCTCCT	Ranieri et al. 2015
FGFR3-IIIb	TCAAGTCCTGGATCAGTGAGAGT	AGGAAGAAGCCCACCCCG	Tomlinson et al. 2005
FGFR3-IIIc	GAGTTCCACTGCAAGGTGTACAGT	GAGAGAACCTCTAGCTCCTTGTCG	Tomlinson et al. 2005

PART II: Determining the role of islet innervation in serotonergic signaling to the pancreas

INTRODUCTION

Since many patients with Type II diabetes become insulin-dependent in the later stages of their disease, finding ways to increase beta-cell mass endogenously is a helpful path to pursue for better diabetes treatments. To do this, we need to understand the mechanisms by which beta cells proliferate and see if we can induce these pathways *in vivo.* Two independent studies found that selective serotonin reuptake inhibitors (SSRIs) increase beta-cell proliferation.[98,99] One, using high throughput screening in larval zebrafish, found that paroxetine (Paxil) induced beta-cell proliferation and confirmed that another SSRI, fluoxetine (Prozac) as well as serotonin (5HT) itself increased beta-cell proliferation.[98] The other used juvenile fish of the FUCCI transgenic line and discovered that two different serotonin uptake inhibitors, Trazadone and Lofepramine, increased beta-cell proliferation.[99] These results make serotonin signaling to zebrafish beta cells an interesting candidate to study for manipulation of beta-cell proliferation.

Serotonin has been implicated before in processes outside the brain. For example, in zebrafish, *tph1b*, the rate limiting enzyme in serotonin synthesis from tryptophan, is expressed in connective tissue progenitor cells after amputation of the tail fin.[100] Serotonin has been shown to be produced by human beta cells in order to communicate with alpha cells to better control blood glucose.[101] In addition, serotonin has been seen in mammals to induce beta-cell proliferation during pregnancy – the beta cells of pregnant mice synthesize serotonin, release that serotonin, and it feeds back on serotonin receptors on beta cells themselves to induce cell cycle progression as well as increasing glucose-stimulated insulin secretion.[102,103]

Since RNA-seq work that has been previously published suggests that zebrafish beta cells do not express any isoform of tryptophan hydroxylase,[18] which is necessary for serotonin synthesis,[104] zebrafish beta cells must not be able to synthesize and release their own serotonin. We had two main hypotheses for where this source of serotonin signaling to the larval zebrafish principal islet could be – either serotonergic neurons communicating with the islet by innervation or neuroendocrine cells releasing serotonin into the bloodstream. Multiple types of innervation to the pancreas is well-studied in mammals. Sympathetic and parasympathetic innervation from the autonomic nervous system is known to influence both beta-cell mass and glucose-stimulated insulin secretion.[105-107] And loss of sympathetic nerves to the islets has been associated with Type I diabetes.[108] Innervation by both sensory nerves[106] and the enteric nervous system[109] has also been established in the mammalian pancreas. Since innervation to the pancreas has been characterized in mammalian systems, we decided to start here in looking for how a serotonergic signal is communicated to the zebrafish principal islet.

We were able to establish that, as in mammals, there is innervation of the larval zebrafish principal islet. Using the *colourless* mutant line as a model of reduced innervation to the islet, we tested whether this innervation was necessary to see proliferation of beta cells in response to an SSRI. Surprisingly, beta cells increased their proliferation in response to Paxil even in the mutant larvae with greatly reduced innervation. This raises some interesting questions about how serotonergic signaling to the pancreas works in zebrafish and whether we are able to use that system as a way to manipulate beta-cell mass.

METHODS

Zebrafish husbandry and lines

Zebrafish were maintained in system water according to standard methods (Westerfield, 2007). All work involving zebrafish was reviewed and pre-approved by the institutional care and use committee. The following previously published lines were used for experiments: *Tg(ptf1a:GFP)*,[110] *Tg(NeuroD:GFP)*,[63] *sox10* mutant line (*colourless*, t3 allele),[111,112] *Tg(ins:hmgb1-GFP)*,[62] *Tg(-28.5sox10:cre; elfa:flox-dsRed-flox-GFP*) (known as *sox10* lineage tracing), and *Tg(tph2:epNTR-RFP)jf41*.[113]

Drug treatment

Paxil (paroxetine hydrochloride hemihydrate Sigma Aldrich P9623) was stored at 10 mM in DMSO at -20 °C and diluted to 10 uM in E3 for treatment. 100% DMSO was stored at room temperature and diluted to 0.1% in E3 for treatment. Edu (5-Ethynyl-2'-deoxyuridine Sigma Aldrich 900584) was stored at 10 mM in PBS at -20 °C and diluted to 500 uM in E3 for treatment. For their 48-hour treatment, larvae were divided into a 24-well plate with a maximum of 5 fish per well. E3 with Edu and either Paxil or DMSO at the above concentrations was added. Plates were kept protected from light and in an incubator at 29 °C for 48 hours. The larvae were then immediately fixed as described below.

Staining and imaging of pancreata

Larvae were fixed in 4% PFA (diluted from 32% in PBS) in glass vials at 4 °C from overnight to a maximum of 2 days. PFA was removed and larvae were rinsed two

times with PBST. The pancreas with the gut attached was dissected out from individual larvae by first removing the head and tail using a razor blade on top of a glass coverslip, then putting these midbodies into PBST overlying a layer of 1% agarose. The gut and pancreas were dissected out using pulled glass needles. These samples were then optionally rinsed one time in 100% MeOH and stored in 100% MeOH at -20 °C until staining continued (except for the Edu staining in which case this is a necessary step). As adapted from Kimmel and Meyer,[114] if samples were stored in MeOH, samples were rehydrated with 5 min incubations in 75% MeOH/25% PBST, then 50% MeOH/50% PBST, then 25%MeOH/75% PBST, then 3 washes in PBST. Samples were incubated at room temperature for 20 minutes in 1% DMSO/0.5% Triton (in PBS) and washed with PBST. For Edu staining, the Click-It reaction was then performed by combining reagents from the Click-iT Edu Alexa Fluor 647 Imaging Kit (Invitrogen C10340) as per Kimmel and Meyer,[114] adding 100 uL (per 1.5 mL Eppendorf) of the staining solution to the samples after removing as much PBST as possible, and incubating for 2 hours in the dark at room temperature. Samples were rinsed 3 times in PBST and then blocked for at least one hour at room temperature (protected from light as the Click-It reaction is light sensitive) in either 1% DMSO / 1% Triton / 2% Goat Serum / 0.1% BSA (in PBS) or 1% DMSO / 1% Triton / 5% Goat Serum (in PBS) depending on the quality of the BSA (some types react with secondary antibodies). Samples were then incubated overnight at 4 °C in primary antibody diluted in blocking solution as per **Supplementary Table 1**. Samples were then washed in either 1% BSA / 0.3% Triton (in PBS) or PBST (depending on the quality of the BSA – see above) 6 times at room temperature for 15 minutes each and then incubated overnight at 4 °C in secondary antibody diluted in blocking solution

as per **Supplementary Table 1**. Samples were washed 6 times at room temperature for 15 minutes each in PBST and then mounted for imaging by placing each sample onto a glass coverslip using forceps, letting excess PBST evaporate, sealing the coverslip to a slide using vacuum grease, then adding back water and sealing the outside with fluorescence mounting media (Dako S3023).

Samples were imaged on a Nikon A1-si Laser Scanning Confocal microscope and when necessary cells were counted using ImageJ. All images in figures are maximum intensity projections of the Z-stacks collected. Analysis of the percent volume of innervation per islet was performed using IMARIS – briefly, the outline of the principal islet in a Z-stack projection was identified by hand and IMARIS was used to calculate the volume of that islet and recognize and calculate the volume of the acetylated tubulin staining within the islet. The ratio of acetylated tubulin volume / islet volume (times 100 to get the percentage) is represented in the figure.

RESULTS

Because of our interest in 5HT signaling to the pancreas and the fact that the gut is the largest producer of 5HT in the body,[115] we wanted to know if we could manipulate serotonergic neurons in the gut. A recent publication suggested that 5HT+ positive neurons in the gut are also *ptf1a*+.[116] But when we did our own staining of guts from *Tg(ptf1a:GFP)* fish we saw that while there are 5HT+ positive cells in the gut wrapped with axons (marked by acetylated tubulin staining) that are assumedly serotonergic neurons (**Figure 1A,B**), these cells do not overlap with *ptf1a* expression (**Figure 1C**).

Even though we don't have an easy marker for serotonergic neurons in the gut, we wanted to move forward with the hypothesis that these cells are the source of 5HT signaling to the pancreas. In order for serotonergic neurons in the gut to signal the islet, the islet of the zebrafish has to be innervated. To look at the presence of innervation in the zebrafish principal islet we used the *Tg(NeuroD:GFP)* line to mark all endocrine cells, and therefore visualize the entire principal islet, and acetylated tubulin staining to mark axons. At 2 days post fertilization (dpf), there is acetylated tubulin staining running next to the principal islet but not within (**Figure 2A**). The small amount of red staining seen within the islet is because acetylated tubulin also marks cilia and beta cells are ciliated. In comparison, at 4 dpf there is now a larger bundle of nerves running at the junction between the gut and the pancreas (see white arrows) and a large amount of innervation, marked by red acetylated tubulin staining, within the principal islet (**Figure 2B**). This timing of innervation is consistent with a recently published similar study.[117] Because previously we've seen SSRIs and serotonin itself able to induce beta-cell proliferation between 3 and 5 dpf,[98] the presence of innervation of the principal islet appearing by 4 dpf is consistent with the hypothesis that innervation of the islet is a possible source of serotonin signaling.

When we looked later in development, endocrine cells differentiating first and then innervation following was also true in the case of secondary islets. Using the same *Tg(NeuroD:GFP)* line to mark endocrine cells and acetylated tubulin staining to show axons, we saw that at 6 dpf secondary islets were present, the principal islet was highly innervated, but there was no acetylated tubulin staining in the secondary islets (shown

best in the magnified inset) (**Figure 2C**). By 7 dpf, the secondary islets were innervated, shown by acetylated tubulin staining through the secondary islet (**Figure 2D**).

Since we now know that the principal islet of the zebrafish is innervated, we next wanted to see whether this innervation was necessary for the proliferative effects of Paxil. In order to do this, we needed a model without innervation of the pancreas. We turned to the well-described *sox10* mutant zebrafish, known as *colourless*, in which neural crest cells apoptose as they migrate, which should result in a lack of an enteric nervous system.[118] In order to look at innervation in *sox10* mutant zebrafish we bred in the *Tg(ins:hmgb1-GFP)* line that marks beta-cell nuclei and then stained for acetylated tubulin as a marker for axons. Instead of genotyping the larvae of a $sox10^{+/-}$ incross, we phenotyped using the fact that homozygous mutants lack melanocytes and are therefore completely colorless.[118] Anything that lacked melanocytes at 2 dpf or later was deemed $sox10^{-/-}$, or homozygous mutant, and anything with the normal melanocyte pattern was deemed $sox10^{+/?}$, which represents a mix of *sox10* heterozygotes and wildtypes. When we examined innervation by acetylated tubulin staining at 5 dpf, we saw that while innervation was present in the gut of both *sox10* mutants and their non-mutant siblings, innervation to the principal islet (marked by the green nuclei of beta cells from *Tg(ins:hmgb1-GFP)*) was markedly reduced in the *sox10* mutants (**Figure 3A,B**). This can be seen especially well when only the acetylated tubulin channel is visualized (**Figure 3A, B, right panels**). We then quantified this difference in innervation between mutants and their non-mutant siblings using IMARIS to calculate the percent of the principal islet that was innervation by volume. This quantification confirmed that $sox10^{-/-}$ larvae have a significantly reduced innervation of the principal islet at 5 dpf (**Figure 3C**).

This reduction in innervation in *sox10* mutants has also been confirmed independently in a recent publication.[117]

These *sox10*$^{-/-}$ mutants seemed like a good model to test the necessity of innervation for the effects of Paxil, but we needed to make sure that a reduction in innervation to the principal islet was the only pancreas phenotype of *sox10*$^{-/-}$ mutants. If the loss of *sox10* caused another functional problem with the islet, that could skew the results we get in terms of the effect of Paxil on beta cells. To get an idea of the role of *sox10*-derived cells in the pancreas we used the lineage tracing line *Tg(-28.5sox10:cre ; elfa:flox-dsRed-flox-GFP*). In this line, any cell that ever expresses *sox10* will then express GFP and so will all of its progeny. When we looked at the gut and the pancreas at 5 dpf, we saw many *sox10*-derived cells closely associated with the enteric nervous system, marked by acetylated tubulin staining (**Figure 4A**). These *sox10*-derived cells were also present and closely associated with axons where innervation branched off into the pancreas (**Figure 4B**). Finally, we sometimes saw *sox10*-derived cells actually adjacent to the principal islet, marked by insulin staining in white, although this was a rare phenomenon (**Figure 4C**).

Because Schwann cells are neural crest-derived and sox10 is an important transcription factor in neural crest cell survival, we hypothesized that these *sox10*-derived cells we saw adjacent to the principal islet were part of a Schwann cell sheath. A Schwann cell sheath around islets has been described previously in mammals[119,120] but never in zebrafish. We used the *Tg(ins:hmgb1-GFP*) line to show beta-cell nuclei and S100ß staining as a marker of both myelinating and unmyelinating Schwann cells. In both *sox10* mutants and their non-mutant siblings, there are Schwann cells surrounding

the principal islet at 5 dpf (**Figure 4D,E**). This means that even though *sox10* mutant zebrafish lose some of their neural crest cells by apoptosis, there is a compensating factor so that important neural crest-derived components like a Schwann cell sheath around the principal islet are still present. Interestingly, in some samples it looked like this Schwann cell sheath was in the process of degradation (**Supplementary Figure 1**). This phenomenon was much more common in *sox10*$^{-/-}$ larvae than their non-mutant counterparts. It will be interesting to follow up on whether this is an antibody artifact or real degradation of the Schwann cell sheath that might be linked to the amount of innervation to the principal islet. We did confirm that this S100ß staining was not a non-specific marker of another endocrine cell type by showing there is no overlap between anti-GFP and anti-S100ß staining in the principal islets of *Tg(NeuroD:GFP)* larvae (**Supplementary Figure 2**). We should investigate though whether these *sox10*+ positive cells could be neurons as a recent publication described *sox10*-derived migrating neurons surrounding the principal islet early in development that are necessary for establishing innervation of the islet.[117]

Since we confirmed that *sox10* mutant zebrafish have reduced innervation of the principal islet compared to their non-mutant siblings and that they appear to still retain other important neural crest-derived components in the pancreas like the Schwann cell sheath surrounding the principal islet, we can use this model to test whether innervation is necessary for the proliferative effects of Paxil. We again used the *Tg(ins:hmgb1-GFP)* line to mark beta-cell nuclei. Larvae were screened for their *sox10* phenotype at 2 dpf and then treated from 3 dpf to 5 dpf with either 0.1% DMSO or 10 uM Paxil as well as Edu (**Figure 5A**). Any cells that proliferated during this 48-hour time period will have taken

up Edu and therefore can be stained and marked as proliferating. When the principal islets were imaged after this 2-day treatment, we saw that in both the *sox10* mutants and their non-mutant siblings there were more cells with overlapping GFP and Edu staining when the larvae had been treated with Paxil versus DMSO (**Figure 5B**). Although there was a high level of variation within each genotype and treatment in terms of the number of proliferating cells, quantifying across samples shows this statistically significant increase in the number of proliferating beta cells in both $sox10^{-/-}$ and $sox10^{+/?}$ larvae when treated with Paxil versus DMSO (**Figure 5C**).

DISCUSSION

By using the *sox10* mutant model we were able to better understand the relationship between innervation to the principal islet of the zebrafish and the effect of SSRIs on beta-cell proliferation – while *sox10* mutant zebrafish have greatly reduced innervation to the islet, their beta cells still proliferate in response to Paxil. This result leads us in two different directions – whether *sox10* is truly the right model to assess the question, and then what other sources of serotonin to the pancreas might be.

When we examined innervation to the principal islet of *sox10* mutants at 5 dpf, we saw that while that innervation was greatly reduced, there were still some residual nerve fibers (**Figure 5**). It is possible that this small amount of remaining innervation is enough to communicate a serotonergic signal and so these nerves are truly necessary for the effects of SSRIs on beta cells. In order to test this, we need a more complete model of loss of innervation to the islet. The first promising lead for an absolute lack of innervation is the *tfap2a;foxd3* double mutant. It has been described that while individual mutants for

these genes have a partial reduction in neural crest-derived cells, the double mutant has a complete loss of neural crest cells early on in development resulting in a variety of defects including loss of melanocytes, malformed craniofacial structure, and a complete absence of peripheral neurons, including the enteric nervous system.[121]

Another mutant line to assess in the future is the *ret* heterozygous mutant line. This fish is a model of the human Hirschsprung Disease in which neural crest cells are unable to populate the developing gut and therefore there is no enteric nervous system. It has been found that *ret* is required in a dose-dependent manner for the enteric nervous system to exist normally[122] and that *ret* heterozygous mutants have a reduced enteric nervous system that can become even more severely reduced by crossing with a *mapk10* mutant line.[123] Both this mutant line and the *tfap2a;foxd3* mutant line should be assessed in the future for whether there is a more complete loss of innervation of the principal islet than what we saw in the *sox10* mutants. If we still see the proliferative effects of Paxil on beta cells when there is an absolute loss of innervation, then we can say with more confidence that innervation (and therefore serotonergic neurons of the gut) is not the source of serotonin signaling to the pancreas.

If the nervous system is not responsible for conveying a serotonin signal to the pancreas, the next candidate to check is the circulatory system, specifically that serotonin is produced by enterochromaffin cells in the gut and travels as an endocrine hormone through the blood to reach the principal islet. Enterochromaffin cells are a specialized population of enteroendocrine cells that reside amongst the epithelial enterocytes of the gut.[124] These cells express *TPH1* (in mammals), synthesize serotonin, and release that serotonin into the circulatory system.[124-126] While very well characterized in mammals,

the role of enterochromaffin cells, and genes we can use as their markers, are not well characterized in the zebrafish. It has been shown previously that the fate of secretory cells (versus enterocytes) in the zebrafish gut is dependent on inhibition of Notch signaling by microbiota[127] and also the acheate-scute like family member *ascl1a*.[128] In addition, enteroendocrine cells in general express *nkx2.2a*.[127] If we can better characterize enterochromaffin cells in zebrafish, then we can manipulate them to understand their role in serotonergic signaling to the pancreas.

Enterochromaffin cells must express one of the zebrafish isoforms of tryptophan hydroxylase which performs the rate-limiting step in the synthesis of 5HT from tryptophan.[104] We saw no *tph2* expression in the gut (**Supplementary Figure 3**), leaving only the isoforms *tph1a* and *tph1b* to pursue further. If we can establish one of these genes as a marker for enterochromaffin cells in the zebrafish gut and manipulate them using an MTZ/NTR ablation system,[32] for example, we could establish if they are the source of serotonergic signaling to the principal islet. Since enterochromaffin cells release serotonin into the blood, we can also test whether the circulatory system is necessary for the effects of Paxil. The well-characterized *cloche* mutant line lacks many parts of the circulatory system, including blood vessels to the pancreas,[129] because *cloche* is necessary for the differentiation of endothelial cells.[130,131] This lack of blood supply to the islet could help us understand whether 5HT is acting as a hormone being transported by blood to beta cells. Finally, if it is the circulatory system that is supplying 5HT to the islet to have an effect on beta cells, they should express serotonin receptors to respond. We are currently working on developing and characterizing a CRISPR-generated mutant of *htr2b* which is the only serotonin receptor expressed in the zebrafish beta cell (at least

in adults),[18] to see whether it is necessary for responding to Paxil. All of the above proposed experiments will help hone in on the mechanism by which serotonin signaling affects the principal islet.

Even if we understand how SSRIs are able to have an effect on beta cells in zebrafish, there is still the question of whether this will translate to humans. There have been several recent studies looking both retrospectively at medical records and also working with cell culture to try to understand the effect of SSRIs on diabetes in a clinical setting. Retrospective studies have actually linked prolonged use of SSRIs, especially in young adults, with an increased risk of developing Type II Diabetes.[132,133] And another study found that in diabetic patients, SSRI use was associated with an increased risk of becoming insulin dependent.[134] Experiments conducted in cell culture suggested that SSRIs cause reduced glucose-stimulated insulin secretion from beta cells, as well as other functional issues in beta cells like problems with cell-cell adhesion, decreased calcium release, increased oxidative damage, and increased apoptosis.[135-137] But there are other retrospective studies that conflict with these results – one that suggests that the link seen between diabetes risk and SSRI use is not causal because they saw no difference in either fasting plasma glucose or HbA1c between patients who did or did not take antidepressants.[138] And finally, several studies actually recommend the use of SSRIs in patients with diabetes and comorbid depression because the use of antidepressants is associated with both a decrease in depressive symptoms as well as better indices of glycemic control like fasting glucose and HbA1c.[139-141] Taken together, these studies suggest that while long-term use of antidepressants is associated with an increased risk of diabetes, this may not be causal and retrospective studies do not have the nuance to be

able to separate out the mental health symptoms, intended and side effects of SSRIs, and metabolic disease. If we can better understand the mechanism behind serotonergic signaling to beta cells in the zebrafish, maybe we can bypass the use of an SSRI and instead find a drug with a more direct effect and fewer complicating side effects.

Finally, there is the interesting question of what the role of serotonergic signaling to the pancreas was originally intended for in the zebrafish. If this signaling is coming from the gut, it could be a way for the gut to communicate with the endocrine cells of the islet post-prandially in preparation for the insulin that will be required for increased blood sugar after a meal. There are a few established facts that support this hypothesis. It is known that feeding, and especially over-nutrition, causes an increase in beta-cell number in the larval zebrafish.[142] In addition, enterochromaffin cells will release serotonin after a meal.[143] And finally, there is recent work showing a link between enterochromaffin cells and beta cells – microbiota in the gut are necessary for the normal development of both the principal islet and secretory cells of the zebrafish gut.[127,144] Taken together, these data suggest the interesting hypothesis that there is a communication between enterochromaffin cells and beta cells post-prandially to better control the rise in blood sugar after food intake.

In conclusion, we saw that although the zebrafish principal islet is innervated, this innervation is not necessary for the proliferative effect that SSRIs have on beta cells. Future work needs to define the mechanism by which serotonergic signaling to the pancreas happens so that eventually we can target it as a means of increasing beta-cell number in the clinic.

Figure 1. Serotonergic neurons in the gut are not *ptf1a*+ (A) Tail of the gut from a 5 dpf *Tg(ptf1a:GFP)* zebrafish larva. Blue is DAPI staining, green is anti-GFP, red is anti-5HT, white is anti-acetylated tubulin (as a marker for axons). (B) Same as above but without DAPI for a clearer view of acetylated tubulin. Yellow arrows mark 5HT+ cells wrapped in acetylated tubulin, representing serotonergic neurons. (C) Same as (A) but only showing 5HT+ and *ptf1a*+ cells. Note there is no overlap between these two cell types.

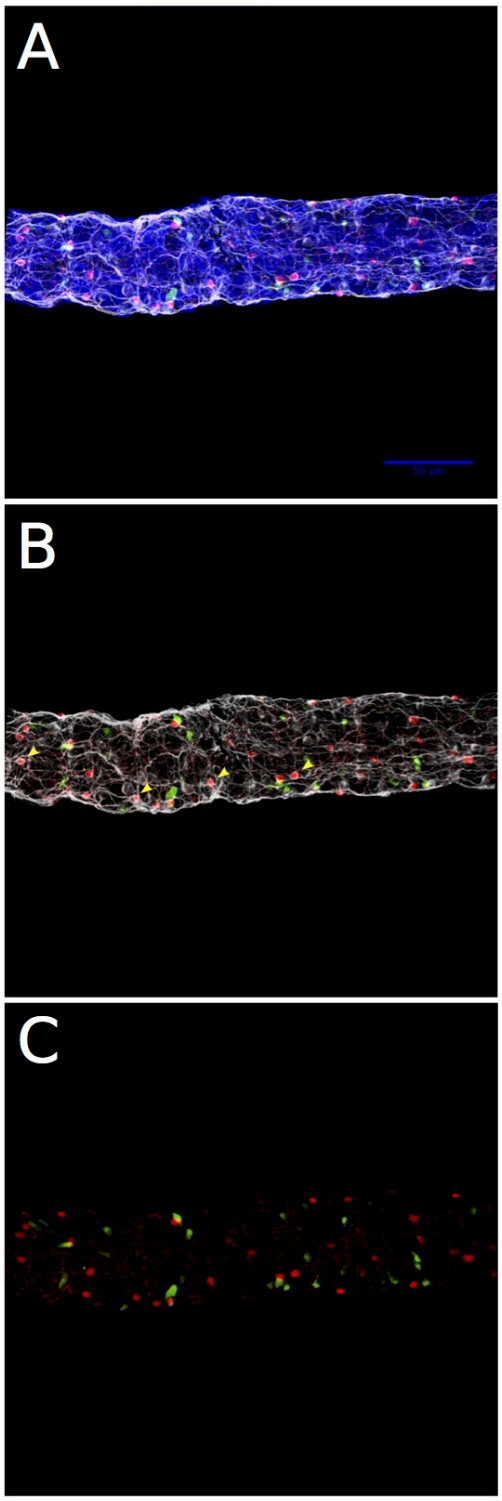
A
B
C

Figure 2. Innervation of islets appears after differentiation. All larvae are *Tg(NeuroD:GFP)*. Blue is DAPI, green is anti-GFP, red is anti-acetylated tubulin (A) Principal islet from a 2 dpf larva. Note the lack of innervation (acetylated tubulin staining) within the islet. (B) Principal islet from a 4 dpf larva. Note the large amount of acetylated tubulin staining, representing innervation, within the islet. White arrows mark acetylated tubulin staining running along the junction between the pancreas and the gut. (C) Gut and pancreas from a 6 dpf larva. A secondary islet is circled and the inset is a slightly zoomed view to show lack of acetylated tubulin staining. (D) Gut and pancreas from a 7 dpf larva. A secondary islet is circled and the inset is a slightly zoomed view to show a nerve fiber running through this islet.

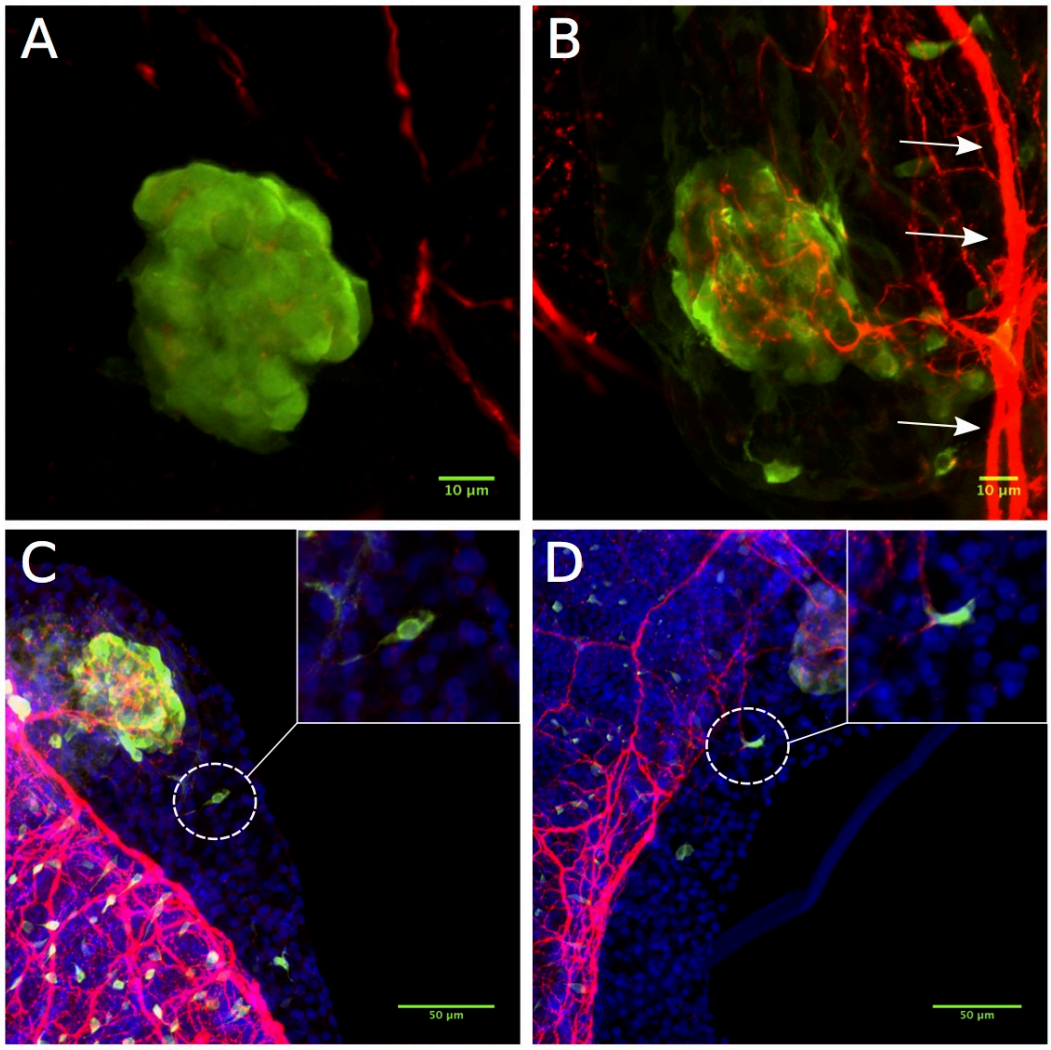
A
10 µm
B
10 µm
C
50 µm
D
50 µm

Figure 3. *sox10* mutant larvae have reduced innervation compared to their non-mutant siblings. Both larvae are *Tg(ins:hmgb1-GFP)*. Green is anti-GFP, red is anti-acetylated tubulin (A) The principal islet from a $sox^{+/?}$ (either heterozygous or wildtype) larva at 5 dpf. The panel on the right is showing just acetylated tubulin staining. Note the large amount of innervation to the principal islet. (B) The principal islet from a $sox10^{-/-}$ larva at 5 dpf. The panel on the right is showing just acetylated tubulin staining. Note the greatly reduced amount of innervation compared to the non-mutant larva. (C) Quantification of the amount of innervation to the principal islet at 5 dpf (percent by volume). Each dot represents the percent innervation from the islet of an individual larva from the clutch of one group mating incross. Welch's t-test. * is a p value of 0.0137.

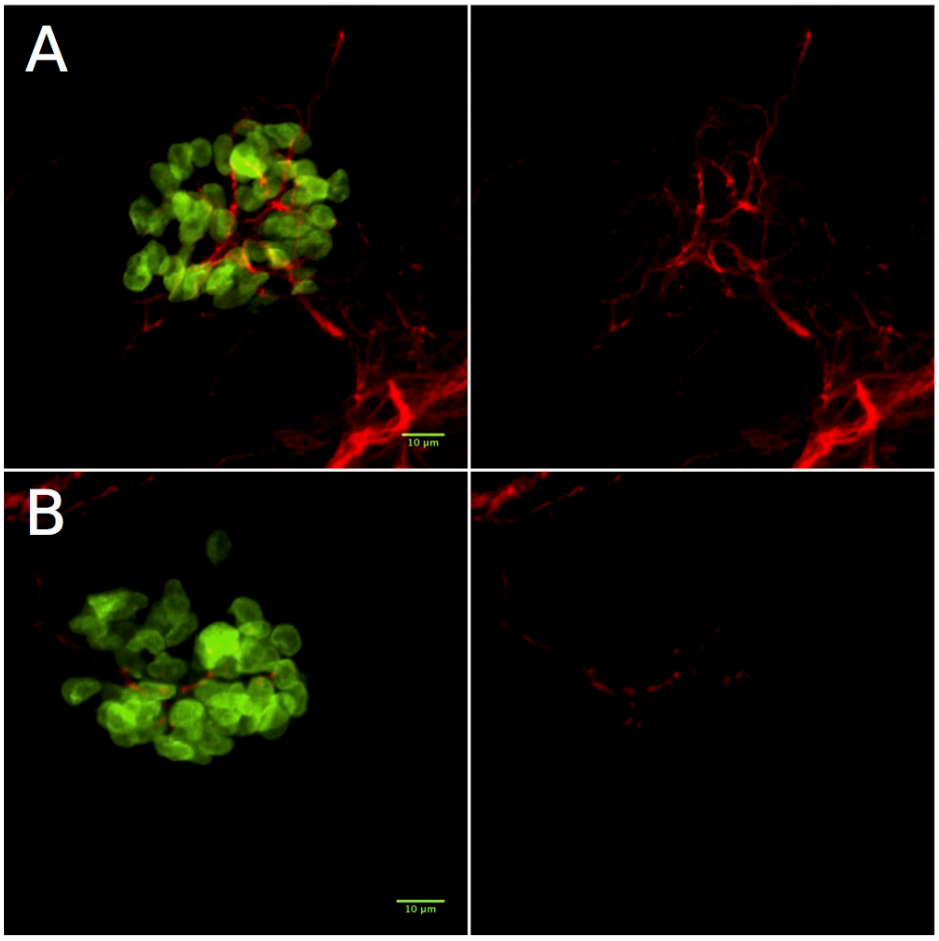
A
10 µm
B
10 µm

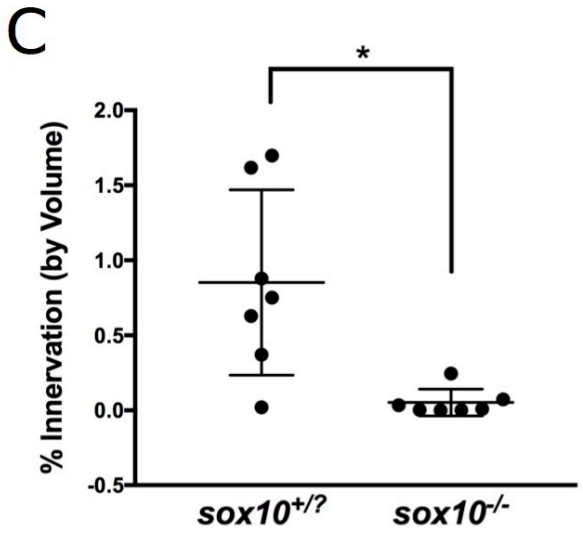
C
*
% Innervation (by Volume)
2.0
1.5
1.0
0.5
0.0
-0.5
sox10+/?
sox10-/-

Figure 4. *sox10*-derived cells are rarely in the pancreas and all *sox10* genotypes have a Schwann cell sheath. (A) The gut and pancreas from a 5 dpf sox10 lineage tracing larva. Green is anti-GFP (*sox10*+), red is anti-acetylated tubulin, white is anti-insulin. The pancreas is outlined in yellow. Notice the association of *sox10*+ cells with the enteric nervous system. (B) Close-up of the principal islet from the same line and staining as above. Notice the *sox10*+ cells associated with the axons branching into the islet. (C) Same as (B). Note the presence of *sox10*+ cells around the principal islet. (D) Principal islet from a 5 dpf *Tg(ins:hmgb1-GFP)* larva that is not mutant for *sox10* (*sox10*$^{+/?}$). Green is anti-GFP and red is anti-S100ß (Schwann cell marker). There appears to be a Schwann cell sheath surrounding the principal islet. (E) Principal islet from a 5 dpf *Tg(ins:hmgb1-GFP)* larva that is *sox10*$^{-/-}$. Note that a Schwann cell sheath is present in this *sox10* mutant as well.

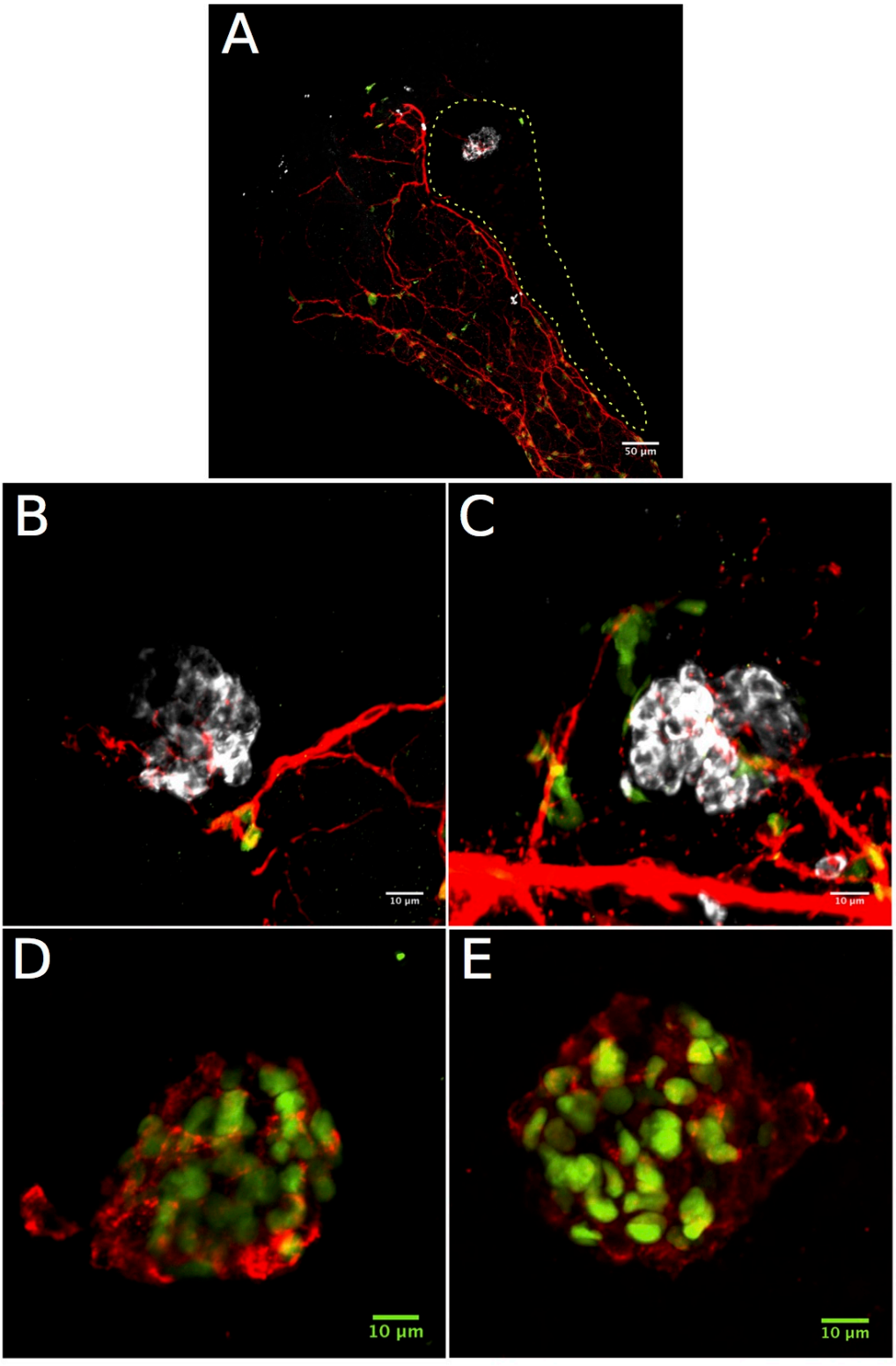
A
50 µm
B
10 µm
C
10 µm
D
10 µm
E
10 µm

Figure 5. *sox10*$^{-/-}$ larvae are still able to respond to Paxil treatment with beta-cell proliferation. (A) Timeline of the experiment showing when fish were crossed, screened, treated, and fixed for assessment. Dpf is days post fertilization. (B) Principal islets from *sox10*$^{+/?}$ and *sox10*$^{-/-}$ larvae (in *Tg(ins:hmgb1-GFP)*) treated with either 0.1% DMSO or 10 uM Paxil. Blue is DAPI, green is anti-GFP, red is Edu. Note the increased amount of yellow (overlap of green and red) in both larvae treated with Paxil (versus DMSO). (C) Quantification of the number of Edu+ (proliferating) beta cells per principal islet. Genotype and treatment is listed on the X-axis. Each dot represents the result from a principal islet from an individual larva. Samples are combined from fish treated on 4 separate occasions. Student's t-test. * is a p value < 0.03.

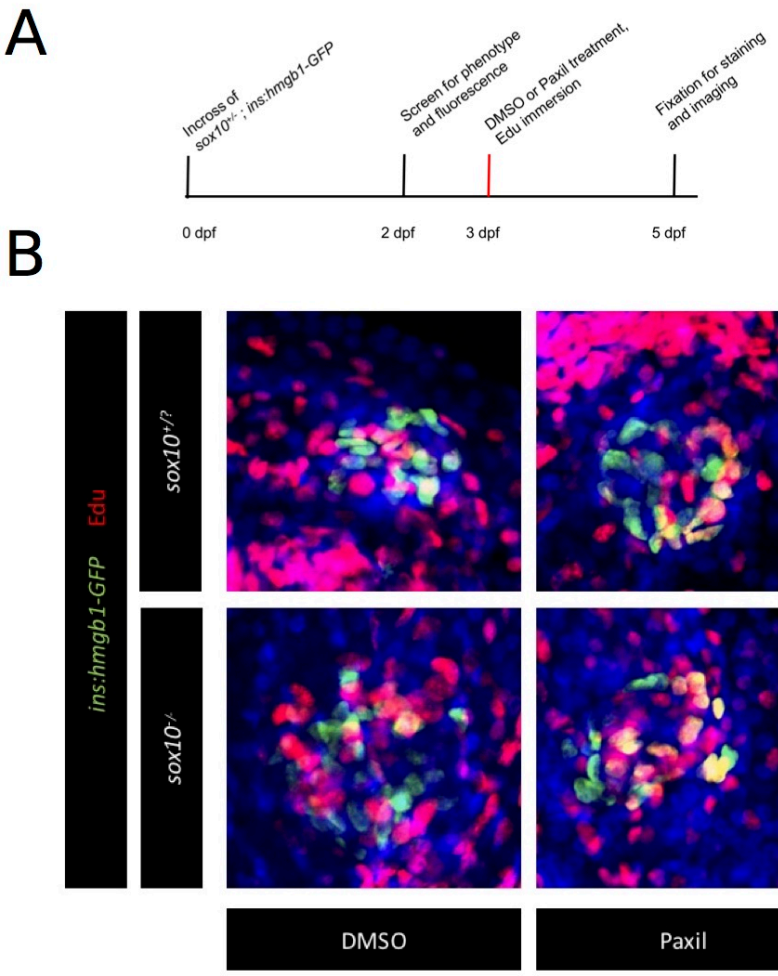
A
Incross of sox10+/- ; ins:hmgb1-GFP
Screen for phenotype and fluorescence
DMSO or Paxil treatment, Edu immersion
Fixation for staining and imaging
0 dpf
2 dpf
3 dpf
5 dpf
B
ins:hmgb1-GFP Edu
sox10+/?
sox10-/-
DMSO
Paxil
C
Edu+ Beta Cell Number
15
10
5
0
*
*
sox10+/? DMSO
sox10+/? Paxil
sox10-/- DMSO
sox10-/- Paxil

Supplementary Figure 1. Principal islet from a *sox10*$^{-/-}$ *; ins:hmgb1-GFP* larva at 5 dpf. Green is anti-GFP and red is anti-S100ß. Note the messy staining that looks like degradation of the Schwann cell sheath.

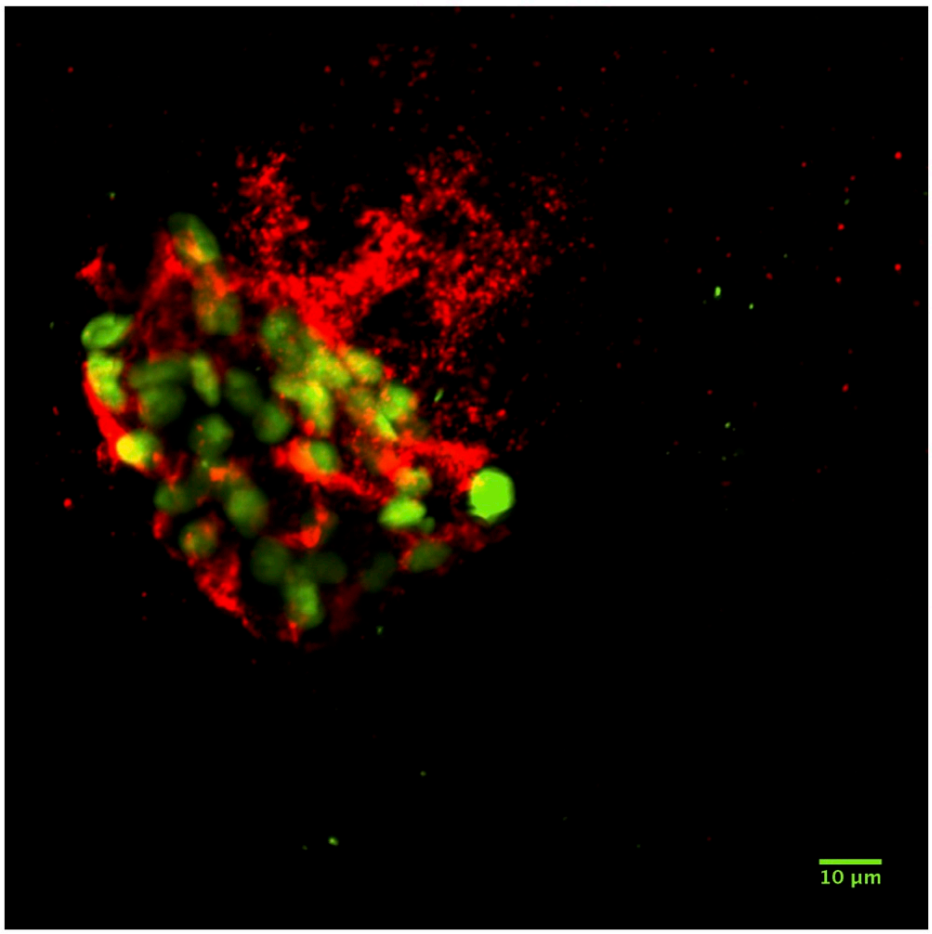
10 µm

Supplementary Figure 2. Principal islet from a *Tg(NeuroD:GFP)* larva at 5 dpf. Green is anti-GFP, red is anti-S100ß, white is anti-insulin. (A) Note how *NeuroD*+ cells do not overlap with S100ß staining, shown with yellow arrows. (B) Note how in the same principal islet insulin staining does overlap with *NeuroD*+ cells, as expected because insulin marks beta cells, an endocrine cell type.

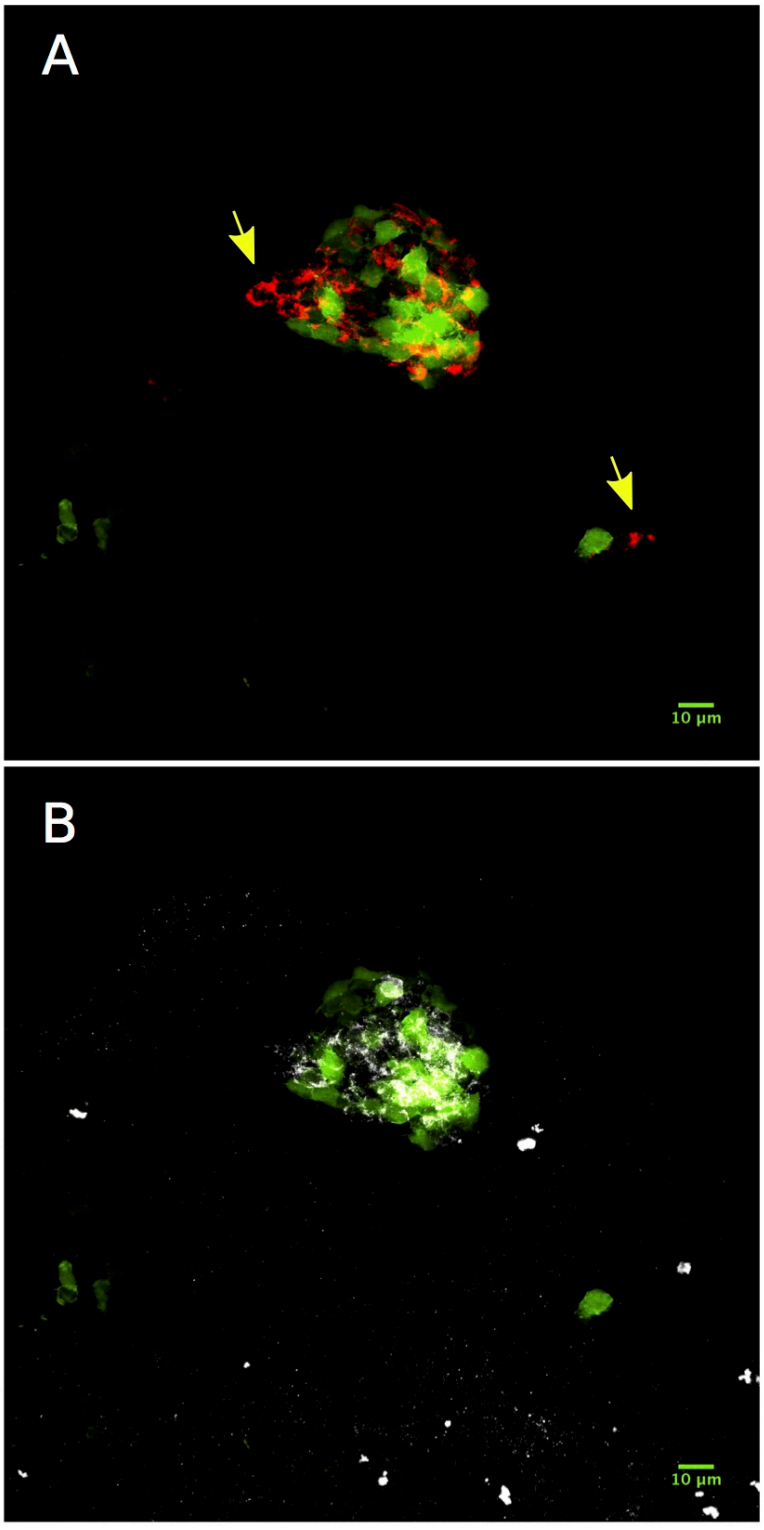
A
10 µm
B
10 µm

Supplementary Figure 3. (A) brain and (B) gut and pancreas from a 5 dpf *Tg(tph2:epNTR-RFP)jf41* larva. Blue is DAPI and red is anti-DsRed. Pancreas is outlined in white. Note the presence of *tph2*+ cells in the brain but not in either the gut or the pancreas.

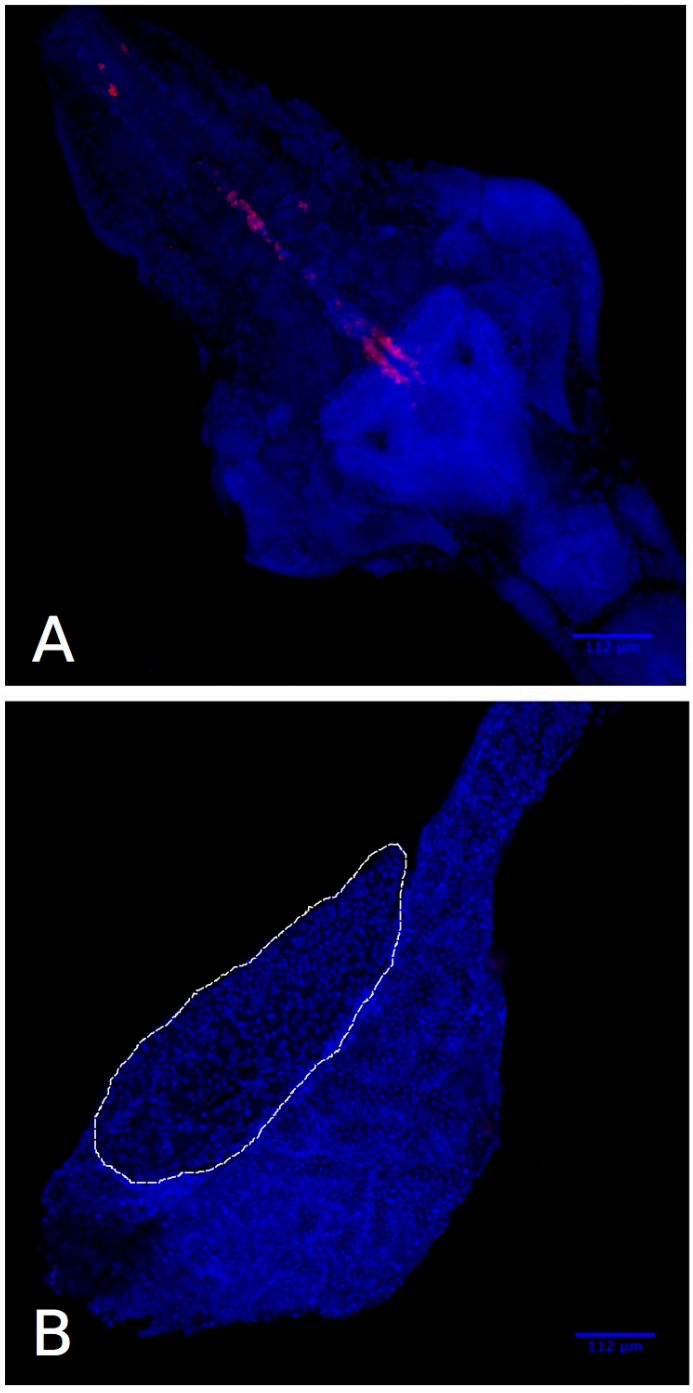
A
112 µm
B
112 µm

Supplementary Table 1 Antibodies Used

	Antibody name	Company	Catalogue Number	Dilution in blocking solution
Primary Antibodies	rabbit anti-GFP	Invitrogen	A11122	1 to 400
	rabbit anti-5HT	Sigma-Aldrich	S5545	1 to 200
	mouse anti-tubulin, acetylated	Sigma-Aldrich	T6793	1 to 400
	rabbit anti-S100 beta [EP1576Y]	abcam	ab52642	1 to 100
	polyclonal guinea pig anti-insulin	Dako	A0564	1 to 200
	Living Colors DsRed Monoclonal Antibody (mouse)	Clontech	632392	1 to 400
Secondary Antibodies	Alexa Fluor 488-conjugated AffiniPure F(ab')2 Fragment Donkey Anti-Rabbit IgG	Jackson ImmunoResearch Laboratories, Inc	711-546-152	1 to 200
	Cy3-conjugated AffiniPure F(ab')2 Fragment Donkey Anti-Rabbit IgG	Jackson ImmunoResearch Laboratories, Inc	711-166-152	1 to 200
	Cy3-conjugated AffiniPure F(ab')2 Fragment Donkey Anti-Mouse IgG	Jackson ImmunoResearch Laboratories, Inc	715-166-150	1 to 200
	Alexa Fluor 647-conjugated AffiniPure F(ab')2 Fragment Donkey Anti-Mouse IgG	Jackson ImmunoResearch Laboratories, Inc	715-606-150	1 to 200
	Alexa Fluor 647-conjugated AffiniPure F(ab')2 Fragment Donkey Anti-Guinea Pig IgG	Jackson ImmunoResearch Laboratories, Inc	706-606-148	1 to 200
	DAPI	Roche	10 236 276 001	stored 5 mg/mL, 1 to 400

BIBLIOGRAPHY

1 Tao, Z., Shi, A. & Zhao, J. Epidemiological Perspectives of Diabetes. *Cell biochemistry and biophysics* **73**, 181-185, doi:10.1007/s12013-015-0598-4 (2015).

2 Stumvoll, M., Goldstein, B. J. & van Haeften, T. W. Type 2 diabetes: principles of pathogenesis and therapy. *The Lancet* **365**, 1333-1346, doi:10.1016/S0140-6736(05)61032-X (2005).

3 Atkinson, M. A., Eisenbarth, G. S. & Michels, A. W. Type 1 diabetes. *Lancet (London, England)* **383**, 69-82, doi:10.1016/S0140-6736(13)60591-7 (2014).

4 Hunter, C. S. & Stein, R. W. Evidence for Loss in Identity, De-Differentiation, and Trans-Differentiation of Islet β-Cells in Type 2 Diabetes. *Frontiers in genetics* **8**, 35, doi:10.3389/fgene.2017.00035 (2017).

5 Valitutto, M. Common crossroads in diabetes management. *Osteopathic medicine and primary care* **2**, 4, doi:10.1186/1750-4732-2-4 (2008).

6 Group, R. S. Relative effectiveness of insulin pump treatment over multiple daily injections and structured education during flexible intensive insulin treatment for type 1 diabetes: cluster randomised trial (REPOSE). *BMJ (Clinical research ed.)* **356**, j1285, doi:10.1136/bmj.j1285 (2017).

7 Maffi, P. *et al.* Risks and benefits of transplantation in the cure of type 1 diabetes: whole pancreas versus islet transplantation. A single center study. *The review of diabetic studies : RDS* **8**, 44-50, doi:10.1900/RDS.2011.8.44 (2011).

8 Moassesfar, S. *et al.* A Comparative Analysis of the Safety, Efficacy, and Cost of Islet Versus Pancreas Transplantation in Nonuremic Patients With Type 1 Diabetes. *American journal of transplantation : official journal of the American Society of Transplantation and the American Society of Transplant Surgeons* **16**, 518-526, doi:10.1111/ajt.13536 (2016).

9 Agulnick, A. D. *et al.* Insulin-Producing Endocrine Cells Differentiated In Vitro From Human Embryonic Stem Cells Function in Macroencapsulation Devices In Vivo. *Stem cells translational medicine* **4**, 1214-1222, doi:10.5966/sctm.2015-0079 (2015).

10 Robert, T. *et al.* Functional Beta Cell Mass from Device-Encapsulated hESC-Derived Pancreatic Endoderm Achieving Metabolic Control. *Stem cell reports* **10**, 739-750, doi:10.1016/j.stemcr.2018.01.040 (2018).

11 Beer, R. L., Parsons, M. J. & Rovira, M. Centroacinar cells: At the center of pancreas regeneration. *Developmental biology* **413**, 8-15, doi:10.1016/j.ydbio.2016.02.027 (2016).

12 Kinkel, M. D. & Prince, V. E. On the diabetic menu: zebrafish as a model for pancreas development and function. *BioEssays : news and reviews in molecular, cellular and developmental biology* **31**, 139-152, doi:10.1002/bies.200800123 (2009).

13 Bastidas-Ponce, A., Scheibner, K., Lickert, H. & Bakhti, M. Cellular and molecular mechanisms coordinating pancreas development. *Development (Cambridge, England)* **144**, 2873-2888, doi:10.1242/dev.140756 (2017).

14 Tiso, N., Moro, E. & Argenton, F. Zebrafish pancreas development. *Molecular and cellular endocrinology* **312**, 24-30, doi:10.1016/j.mce.2009.04.018 (2009).

15 Kopp, J. L. *et al.* Sox9+ ductal cells are multipotent progenitors throughout development but do not produce new endocrine cells in the normal or injured adult pancreas. *Development (Cambridge, England)* **138**, 653-665, doi:10.1242/dev.056499 (2011).
16 Seymour, P. A. *et al.* SOX9 is required for maintenance of the pancreatic progenitor cell pool. *Proceedings of the National Academy of Sciences of the United States of America* **104**, 1865-1870, doi:10.1073/pnas.0609217104 (2007).
17 Delous, M. *et al.* Sox9b is a key regulator of pancreaticobiliary ductal system development. *PLoS genetics* **8**, e1002754, doi:10.1371/journal.pgen.1002754 (2012).
18 Tarifeño-Saldivia, E. *et al.* Transcriptome analysis of pancreatic cells across distant species highlights novel important regulator genes. *BMC biology* **15**, 21, doi:10.1186/s12915-017-0362-x (2017).
19 Xu, X. *et al.* β Cells Can Be Generated from Endogenous Progenitors in Injured Adult Mouse Pancreas. *Cell* **132**, 197-207, doi:10.1016/j.cell.2007.12.015 (2008).
20 Al-Hasani, K. *et al.* Adult Duct-Lining Cells Can Reprogram into β-like Cells Able to Counter Repeated Cycles of Toxin-Induced Diabetes. *Developmental Cell* **26**, 86-100, doi:10.1016/j.devcel.2013.05.018 (2013).
21 Van de Casteele, M. *et al.* Partial Duct Ligation: -Cell Proliferation and Beyond. *Diabetes* **63**, 2567-2577, doi:10.2337/db13-0831 (2014).
22 Xiao, X. *et al.* No evidence for β cell neogenesis in murine adult pancreas. *The Journal of clinical investigation* **123**, 2207-2217, doi:10.1172/JCI66323 (2013).
23 Xiao, X. *et al.* Neurogenin3 Activation Is Not Sufficient to Direct Duct-to-Beta Cell Transdifferentiation in the Adult Pancreas. *The Journal of biological chemistry* **288**, 25297-25308, doi:10.1074/jbc.M113.484022 (2013).
24 Arnes, L., Hill, J. T., Gross, S., Magnuson, M. A. & Sussel, L. Ghrelin Expression in the Mouse Pancreas Defines a Unique Multipotent Progenitor Population. *PloS one* **7**, e52026, doi:10.1371/journal.pone.0052026 (2012).
25 Chera, S. *et al.* Diabetes recovery by age-dependent conversion of pancreatic δ-cells into insulin producers. *Nature* **514**, 503-507, doi:10.1038/nature13633 (2014).
26 Courtney, M. *et al.* The Inactivation of Arx in Pancreatic α-Cells Triggers Their Neogenesis and Conversion into Functional β-Like Cells. *PLoS genetics* **9**, e1003934, doi:10.1371/journal.pgen.1003934 (2013).
27 Nir, T., Melton, D. A. & Dor, Y. Recovery from diabetes in mice by β cell regeneration. *The Journal of clinical investigation* **117**, 2553-2561, doi:10.1172/JCI32959 (2007).
28 Thorel, F. *et al.* Conversion of adult pancreatic α-cells to β-cells after extreme β-cell loss. *Nature* **464**, 1149-1154, doi:10.1038/nature08894 (2010).
29 Meier, J. J., Bhushan, A., Butler, A. E., Rizza, R. A. & Butler, P. C. Sustained beta cell apoptosis in patients with long-standing type 1 diabetes: indirect evidence for islet regeneration? *Diabetologia* **48**, 2221-2228, doi:10.1007/s00125-005-1949-2 (2005).
30 Butler, A. E. *et al.* Modestly increased beta cell apoptosis but no increased beta cell replication in recent-onset type 1 diabetic patients who died of diabetic

ketoacidosis. *Diabetologia* **50**, 2323-2331, doi:10.1007/s00125-007-0794-x (2007).
31 Moss, J. B. *et al.* Regeneration of the pancreas in adult zebrafish. *Diabetes* **58**, 1844-1851, doi:10.2337/db08-0628 (2009).
32 Pisharath, H., Rhee, J. M., Swanson, M. A., Leach, S. D. & Parsons, M. J. Targeted ablation of beta cells in the embryonic zebrafish pancreas using E. coli nitroreductase. *Mechanisms of development* **124**, 218-229, doi:10.1016/j.mod.2006.11.005 (2007).
33 Delaspre, F. *et al.* Centroacinar Cells Are Progenitors That Contribute to Endocrine Pancreas Regeneration. *Diabetes* **64**, 3499-3509, doi:10.2337/db15-0153 (2015).
34 Huang, W. *et al.* Sox9b is a mediator of retinoic acid signaling restricting endocrine progenitor differentiation. *Developmental biology* **418**, 28-39, doi:10.1016/j.ydbio.2016.08.019 (2016).
35 Miyamoto, Y. *et al.* Notch mediates TGFα-induced changes in epithelial differentiation during pancreatic tumorigenesis. *Cancer cell* **3**, 565-576, doi:10.1016/S1535-6108(03)00140-5 (2003).
36 Seymour, P. A. Sox9: a master regulator of the pancreatic program. *The review of diabetic studies : RDS* **11**, 51-83, doi:10.1900/RDS.2014.11.51 (2014).
37 Kopp, J. L. *et al.* Identification of Sox9-dependent acinar-to-ductal reprogramming as the principal mechanism for initiation of pancreatic ductal adenocarcinoma. *Cancer cell* **22**, 737-750, doi:10.1016/j.ccr.2012.10.025 (2012).
38 Wu, Y. *et al.* c-Kit and stem cell factor regulate PANC-1 cell differentiation into insulin- and glucagon-producing cells. *Laboratory Investigation* **90**, 1373-1384, doi:10.1038/labinvest.2010.106 (2010).
39 Cirulli, V. *et al.* KSA antigen Ep-CAM mediates cell-cell adhesion of pancreatic epithelial cells: morphoregulatory roles in pancreatic islet development. *J Cell Biol* **140**, 1519-1534, doi:10.2307/1618545 (1998).
40 Maimets, M. *et al.* Long-Term In Vitro Expansion of Salivary Gland Stem Cells Driven by Wnt Signals. *Stem cell reports* **6**, 150-162, doi:10.1016/j.stemcr.2015.11.009 (2016).
41 Tanimizu, N., Kobayashi, S., Ichinohe, N. & Mitaka, T. Downregulation of miR122 by grainyhead-like 2 restricts the hepatocytic differentiation potential of adult liver progenitor cells. *Development (Cambridge, England)* **141**, 4448-4456, doi:10.1242/dev.113654 (2014).
42 Balzar, M. *et al.* The structural analysis of adhesions mediated by Ep-CAM. *Experimental cell research* **246**, 108-121, doi:10.1006/excr.1998.4263 (1999).
43 Kim, D., Langmead, B. & Salzberg, S. L. HISAT: a fast spliced aligner with low memory requirements. *Nature Methods* **12**, 357-360, doi:10.1038/nmeth.3317 (2015).
44 Robinson, J. T. *et al.* Integrative genomics viewer. *Nature biotechnology* **29**, 24-26, doi:10.1038/nbt0111-24 (2011).
45 Thorvaldsdottir, H., Robinson, J. T. & Mesirov, J. P. Integrative Genomics Viewer (IGV): high-performance genomics data visualization and exploration. *Briefings in Bioinformatics* **14**, 178-192, doi:10.1093/bib/bbs017 (2013).

46 Liao, Y., Smyth, G. K. & Shi, W. The Subread aligner: fast, accurate and scalable read mapping by seed-and-vote. *Nucleic acids research* **41**, e108-e108, doi:10.1093/nar/gkt214 (2013).
47 Love, M. I., Huber, W. & Anders, S. Moderated estimation of fold change and dispersion for RNA-seq data with DESeq2. *Genome Biology* **15**, 31, doi:10.1186/s13059-014-0550-8 (2014).
48 Kuleshov, M. V. *et al.* Enrichr: a comprehensive gene set enrichment analysis web server 2016 update. *Nucleic acids research* **44**, W90-W97, doi:10.1093/nar/gkw377 (2016).
49 Chen, E. Y. *et al.* Enrichr: interactive and collaborative HTML5 gene list enrichment analysis tool. *BMC bioinformatics* **14**, 128, doi:10.1186/1471-2105-14-128 (2013).
50 Lee, T. I., Johnstone, S. E. & Young, R. A. Chromatin immunoprecipitation and microarray-based analysis of protein location. *Nature Protocols* **1**, 729-748, doi:10.1038/nprot.2006.98 (2006).
51 Langmead, B. & Salzberg, S. L. Fast gapped-read alignment with Bowtie 2. *Nature Methods* **9**, 357-359, doi:10.1038/nmeth.1923 (2012).
52 Li, H. *et al.* The Sequence Alignment/Map format and SAMtools. *Bioinformatics* **25**, 2078-2079, doi:10.1093/bioinformatics/btp352 (2009).
53 Zhang, Y. *et al.* Model-based analysis of ChIP-Seq (MACS). *Genome Biology* **9**, R137, doi:10.1186/gb-2008-9-9-r137 (2008).
54 Consortium, T. E. P. An integrated encyclopedia of DNA elements in the human genome. *Nature* **489**, 57-74, doi:10.1038/nature11247 (2012).
55 Shin, H., Liu, T., Manrai, A. K. & Liu, X. S. CEAS: cis-regulatory element annotation system. *Bioinformatics* **25**, 2605-2606, doi:10.1093/bioinformatics/btp479 (2009).
56 Liu, T. *et al.* Cistrome: an integrative platform for transcriptional regulation studies. *Genome Biology* **12**, R83, doi:10.1186/gb-2011-12-8-r83 (2011).
57 Khan, A. *et al.* JASPAR 2018: update of the open-access database of transcription factor binding profiles and its web framework. *Nucleic acids research* **46**, D260-D266, doi:10.1093/nar/gkx1126 (2017).
58 McLean, C. Y. *et al.* GREAT improves functional interpretation of cis-regulatory regions. *Nature biotechnology* **28**, 495-501, doi:10.1038/nbt.1630 (2010).
59 Ishii, H. *et al.* Epithelial splicing regulatory proteins 1 (ESRP1) and 2 (ESRP2) suppress cancer cell motility via different mechanisms. *J Biol Chem* **289**, 27386-27399, doi:10.1074/jbc.M114.589432 (2014).
60 Ranieri, D. *et al.* Expression of the FGFR2 mesenchymal splicing variant in epithelial cells drives epithelial-mesenchymal transition. *Oncotarget* **7**, 5440-5460, doi:10.18632/oncotarget.6706 (2016).
61 Tomlinson, D. C., L'Hôte, C. G., Kennedy, W., Pitt, E. & Knowles, M. A. Alternative splicing of fibroblast growth factor receptor 3 produces a secreted isoform that inhibits fibroblast growth factor-induced proliferation and is repressed in urothelial carcinoma cell lines. *Cancer research* **65**, 10441-10449, doi:10.1158/0008-5472.CAN-05-1718 (2005).

62 Parsons, M. J. *et al.* Notch-responsive cells initiate the secondary transition in larval zebrafish pancreas. *Mechanisms of development* **126**, 898-912, doi:10.1016/j.mod.2009.07.002 (2009).
63 Obholzer, N. *et al.* Vesicular glutamate transporter 3 is required for synaptic transmission in zebrafish hair cells. *The Journal of neuroscience : the official journal of the Society for Neuroscience* **28**, 2110-2118, doi:10.1523/JNEUROSCI.5230-07.2008 (2008).
64 Li, D. *et al.* Adrenocortical zonation factor 1 is a novel matricellular protein promoting integrin-mediated adhesion of adrenocortical and vascular smooth muscle cells. *The FEBS journal* **274**, 2506-2522, doi:10.1111/j.1742-4658.2007.05786.x (2007).
65 Tajiri, Y. *et al.* Tubulointerstitial nephritis antigen-like 1 is expressed in the uterus and binds with integrins in decidualized endometrium during postimplantation in mice. *Biology of reproduction* **82**, 263-270, doi:10.1095/biolreprod.109.080028 (2010).
66 Cui, X. B., Luan, J. N., Ye, J. & Chen, S. Y. RGC32 deficiency protects against high-fat diet-induced obesity and insulin resistance in mice. *The Journal of endocrinology* **224**, 127-137, doi:10.1530/JOE-14-0548 (2015).
67 Schnell, U., Cirulli, V. & Giepmans, B. N. EpCAM: structure and function in health and disease. *Biochim Biophys Acta* **1828**, 1989-2001, doi:10.1016/j.bbamem.2013.04.018 (2013).
68 Chan, S. W., Fowler, K. J., Choo, K. H. & Kalitsis, P. Spef1, a conserved novel testis protein found in mouse sperm flagella. *Gene* **353**, 189-199, doi:10.1016/j.gene.2005.04.025 (2005).
69 Xue, J. C. & Goldberg, E. Identification of a novel testis-specific leucine-rich protein in humans and mice. *Biology of reproduction* **62**, 1278-1284 (2000).
70 Zeng, L. *et al.* Identification of a novel human doublecortin-domain-containing gene (DCDC1) expressed mainly in testis. *Journal of human genetics* **48**, 393-396, doi:10.1007/s10038-003-0033-3 (2003).
71 Bernard, P. *et al.* Dimerization of SOX9 is required for chondrogenesis, but not for sex determination. *Human molecular genetics* **12**, 1755-1765 (2003).
72 He, X., Ohba, S., Hojo, H. & McMahon, A. P. AP-1 family members act with Sox9 to promote chondrocyte hypertrophy. *Development (Cambridge, England)* **143**, 3012-3023, doi:10.1242/dev.134502 (2016).
73 Shih, H. P. *et al.* A Gene Regulatory Network Cooperatively Controlled by Pdx1 and Sox9 Governs Lineage Allocation of Foregut Progenitor Cells. *Cell reports* **13**, 326-336, doi:10.1016/j.celrep.2015.08.082 (2015).
74 Kadaja, M. *et al.* SOX9: a stem cell transcriptional regulator of secreted niche signaling factors. *Genes Dev* **28**, 328-341, doi:10.1101/gad.233247.113 (2014).
75 Zeng, L., Kempf, H., Murtaugh, L. C., Sato, M. E. & Lassar, A. B. Shh establishes an Nkx3.2/Sox9 autoregulatory loop that is maintained by BMP signals to induce somitic chondrogenesis. *Genes & development* **16**, 1990-2005, doi:10.1101/gad.1008002 (2002).
76 Lefebvre, V. & Dvir-Ginzberg, M. SOX9 and the many facets of its regulation in the chondrocyte lineage. *Connective tissue research* **58**, 2-14, doi:10.1080/03008207.2016.1183667 (2017).

77 Lu, H., Ma, J., Yang, Y., Shi, W. & Luo, L. EpCAM is an endoderm-specific Wnt derepressor that licenses hepatic development. *Developmental Cell* **24**, 543-553, doi:10.1016/j.devcel.2013.01.021 (2013).
78 Huang, W. *et al.* Retinoic acid plays an evolutionarily conserved and biphasic role in pancreas development. *Developmental biology* **394**, 83-93, doi:10.1016/j.ydbio.2014.07.021 (2014).
79 Lodh, S., O'Hare, E. A. & Zaghloul, N. A. Primary cilia in pancreatic development and disease. *Birth defects research. Part C, Embryo today : reviews* **102**, 139-158, doi:10.1002/bdrc.21063 (2014).
80 Muto, A., Iida, A., Satoh, S. & Watanabe, S. The group E Sox genes Sox8 and Sox9 are regulated by Notch signaling and are required for Müller glial cell development in mouse retina. *Experimental eye research* **89**, 549-558, doi:10.1016/j.exer.2009.05.006 (2009).
81 Briot, A. *et al.* Repression of Sox9 by Jag1 is continuously required to suppress the default chondrogenic fate of vascular smooth muscle cells. *Developmental Cell* **31**, 707-721, doi:10.1016/j.devcel.2014.11.023 (2014).
82 Capaccione, K. M. *et al.* Sox9 mediates Notch1-induced mesenchymal features in lung adenocarcinoma. *Oncotarget* **5**, 3636-3650, doi:10.18632/oncotarget.1970 (2014).
83 Haller, R. *et al.* Notch1 signaling regulates chondrogenic lineage determination through Sox9 activation. *Cell death and differentiation* **19**, 461-469, doi:10.1038/cdd.2011.114 (2012).
84 Kadaja, M. *et al.* SOX9: a stem cell transcriptional regulator of secreted niche signaling factors. *Genes & development* **28**, 328-341, doi:10.1101/gad.233247.113 (2014).
85 Ohba, S., He, X., Hojo, H. & McMahon, A. P. Distinct Transcriptional Programs Underlie Sox9 Regulation of the Mammalian Chondrocyte. *Cell reports* **12**, 229-243, doi:10.1016/j.celrep.2015.06.013 (2015).
86 Igarashi, T. *et al.* Tubulointerstitial nephritis antigen-like 1 is expressed in extraembryonic tissues and interacts with laminin 1 in the Reichert membrane at postimplantation in the mouse. *Biology of reproduction* **81**, 948-955, doi:10.1095/biolreprod.109.078162 (2009).
87 Wex, T. *et al.* TIN-ag-RP, a novel catalytically inactive cathepsin B-related protein with EGF domains, is predominantly expressed in vascular smooth muscle cells. *Biochemistry* **40**, 1350-1357, doi:10.1021/bi002266o (2001).
88 Favre, C. J. *et al.* Expression of genes involved in vascular development and angiogenesis in endothelial cells of adult lung. *American journal of physiology. Heart and circulatory physiology* **285**, H1917-1938, doi:10.1152/ajpheart.00983.2002 (2003).
89 Kalfa, T. A., Thull, J. D., Butkowski, R. J. & Charonis, A. S. Tubulointerstitial nephritis antigen interacts with laminin and type IV collagen and promotes cell adhesion. *The Journal of biological chemistry* **269**, 1654-1659 (1994).
90 Ueda, J. *et al.* Epithelial splicing regulatory protein 1 is a favorable prognostic factor in pancreatic cancer that attenuates pancreatic metastases. *Oncogene* **33**, 4485-4495, doi:10.1038/onc.2013.392 (2013).

91 Deloria, A. J. *et al.* Epithelial splicing regulatory protein 1 and 2 paralogues correlate with splice signatures and favorable outcome in human colorectal cancer. *Oncotarget* **7**, 73800-73816, doi:10.18632/oncotarget.12070 (2016).
92 Warzecha, C. C., Sato, T. K., Nabet, B., Hogenesch, J. B. & Carstens, R. P. ESRP1 and ESRP2 Are Epithelial Cell-Type-Specific Regulators of FGFR2 Splicing. *Molecular Cell* **33**, 591-601, doi:10.1016/j.molcel.2009.01.025 (2009).
93 González, B., Denzel, S., Mack, B., Conrad, M. & Gires, O. EpCAM Is Involved in Maintenance of the Murine Embryonic Stem Cell Phenotype. *Stem cells (Dayton, Ohio)* **27**, 1782-1791, doi:10.1002/stem.97 (2009).
94 Lu, T.-Y. *et al.* Epithelial Cell Adhesion Molecule Regulation Is Associated with the Maintenance of the Undifferentiated Phenotype of Human Embryonic Stem Cells. *The Journal of biological chemistry* **285**, 8719-8732, doi:10.1074/jbc.M109.077081 (2010).
95 Vercollone, J. R., Balzar, M., Litvinov, S. V., Yang, W. & Cirulli, V. MMTV/LTR Promoter-Driven Transgenic Expression of EpCAM Leads to the Development of Large Pancreatic Islets. *The journal of histochemistry and cytochemistry : official journal of the Histochemistry Society* **63**, 613-625, doi:10.1369/0022155415583876 (2015).
96 Rodrigo-Torres, D. *et al.* The biliary epithelium gives rise to liver progenitor cells. *Hepatology* **60**, 1367-1377, doi:10.1002/hep.27078 (2014).
97 Lorent, K., Moore, J. C., Siekmann, A. F., Lawson, N. & Pack, M. Reiterative use of the notch signal during zebrafish intrahepatic biliary development. *Developmental dynamics : an official publication of the American Association of Anatomists* **239**, 855-864, doi:10.1002/dvdy.22220 (2010).
98 Wang, G. *et al.* First quantitative high-throughput screen in zebrafish identifies novel pathways for increasing pancreatic β-cell mass. *eLife* **4**, 3, doi:10.7554/eLife.08261 (2015).
99 Tsuji, N. *et al.* Whole organism high content screening identifies stimulators of pancreatic beta-cell proliferation. *PloS one* **9**, e104112, doi:10.1371/journal.pone.0104112 (2014).
100 Tornini, V. A. *et al.* Live Monitoring of Blastemal Cell Contributions during Appendage Regeneration. *Current biology : CB* **26**, 2981-2991, doi:10.1016/j.cub.2016.08.072 (2016).
101 Almaça, J. *et al.* Human Beta Cells Produce and Release Serotonin to Inhibit Glucagon Secretion from Alpha Cells. *Cell reports* **17**, 3281-3291, doi:10.1016/j.celrep.2016.11.072 (2016).
102 Kim, H. *et al.* Serotonin regulates pancreatic beta cell mass during pregnancy. *Nature Publishing Group* **16**, 804-808, doi:10.1038/nm.2173 (2010).
103 Ohara-Imaizumi, M. *et al.* Serotonin regulates glucose-stimulated insulin secretion from pancreatic β cells during pregnancy. *Proceedings of the National Academy of Sciences of the United States of America* **110**, 19420-19425, doi:10.1073/pnas.1310953110 (2013).
104 El-Merahbi, R., Löffler, M., Mayer, A. & Sumara, G. The roles of peripheral serotonin in metabolic homeostasis. *FEBS letters* **589**, 1728-1734, doi:10.1016/j.febslet.2015.05.054 (2015).

105 Shirakawa, J., De Jesus, D. F. & Kulkarni, R. N. Exploring inter-organ crosstalk to uncover mechanisms that regulate β-cell function and mass. *Nature Publishing Group* **71**, 896-903, doi:10.1038/ejcn.2017.13 (2017).
106 Lindsay, T. H. *et al.* A quantitative analysis of the sensory and sympathetic innervation of the mouse pancreas. *Neuroscience* **137**, 1417-1426, doi:10.1016/j.neuroscience.2005.10.055 (2006).
107 Prates, K. V. *et al.* Sympathetic innervation is essential for metabolic homeostasis and pancreatic beta cell function in adult rats. *Molecular and cellular endocrinology*, doi:10.1016/j.mce.2017.09.031 (2017).
108 Mundinger, T. O. *et al.* Human Type 1 Diabetes Is Characterized by an Early, Marked, Sustained, and Islet-Selective Loss of Sympathetic Nerves. *Diabetes* **65**, 2322-2330, doi:10.2337/db16-0284 (2016).
109 Kirchgessner, A. L. & Gershon, M. D. Innervation of the pancreas by neurons in the gut. *The Journal of neuroscience : the official journal of the Society for Neuroscience* **10**, 1626-1642 (1990).
110 Godinho, L. *et al.* Targeting of amacrine cell neurites to appropriate synaptic laminae in the developing zebrafish retina. *Development (Cambridge, England)* **132**, 5069-5079, doi:10.1242/dev.02075 (2005).
111 Kelsh, R. N. *et al.* Zebrafish pigmentation mutations and the processes of neural crest development. *Development (Cambridge, England)* **123**, 369-389 (1996).
112 Kelsh, R. N. & Eisen, J. S. The zebrafish colourless gene regulates development of non-ectomesenchymal neural crest derivatives. *Development (Cambridge, England)* **127**, 515-525 (2000).
113 Kawashima, T., Zwart, M. F., Yang, C.-T., Mensh, B. D. & Ahrens, M. B. The Serotonergic System Tracks the Outcomes of Actions to Mediate Short-Term Motor Learning. *Cell* **167**, 933-946.e920, doi:10.1016/j.cell.2016.09.055 (2016).
114 Kimmel, R. A. & Meyer, D. Molecular regulation of pancreas development in zebrafish. *Methods in cell biology* **100**, 261-280, doi:10.1016/B978-0-12-384892-5.00010-4 (2010).
115 Ahlman, H. & Nilsson. The gut as the largest endocrine organ in the body. *Annals of oncology : official journal of the European Society for Medical Oncology* **12 Suppl 2**, S63-68 (2001).
116 Uribe, R. A., Gu, T. & Bronner, M. E. A novel subset of enteric neurons revealed by ptf1a:GFP in the developing zebrafish enteric nervous system. *Genesis (New York, N.Y. : 2000)*, doi:10.1002/dvg.22927 (2016).
117 Yang, Y. H. C., Kawakami, K. & Stainier, D. Y. A new mode of pancreatic islet innervation revealed by live imaging in zebrafish. *eLife* **7**, 393, doi:10.7554/eLife.34519 (2018).
118 Dutton, K. A. *et al.* Zebrafish colourless encodes sox10 and specifies non-ectomesenchymal neural crest fates. *Development (Cambridge, England)* **128**, 4113-4125 (2001).
119 Donev, S. R. Ultrastructural evidence for the presence of a glial sheath investing the islets of Langerhans in the pancreas of mammals. *Cell and Tissue Research* **237**, 343-348 (1984).

120 Sunami, E. *et al.* Morphological characteristics of Schwann cells in the islets of Langerhans of the murine pancreas. *Archives of histology and cytology* **64**, 191-201 (2001).
121 Wang, W.-D., Melville, D. B., Montero-Balaguer, M., Hatzopoulos, A. K. & Knapik, E. W. Tfap2a and Foxd3 regulate early steps in the development of the neural crest progenitor population. *Developmental biology* **360**, 173-185, doi:10.1016/j.ydbio.2011.09.019 (2011).
122 Heanue, T. A. & Pachnis, V. Ret isoform function and marker gene expression in the enteric nervous system is conserved across diverse vertebrate species. *Mechanisms of development* **125**, 687-699, doi:10.1016/j.mod.2008.04.006 (2008).
123 Heanue, T. A. *et al.* A Novel Zebrafish ret Heterozygous Model of Hirschsprung Disease Identifies a Functional Role for mapk10 as a Modifier of Enteric Nervous System Phenotype Severity. *PLoS genetics* **12**, e1006439, doi:10.1371/journal.pgen.1006439 (2016).
124 Bertrand, P. P. & Bertrand, R. L. Serotonin release and uptake in the gastrointestinal tract. *Autonomic Neuroscience: Basic and Clinical* **153**, 47-57, doi:10.1016/j.autneu.2009.08.002 (2010).
125 Gershon, M. D. 5-Hydroxytryptamine (serotonin) in the gastrointestinal tract. *Current opinion in endocrinology, diabetes, and obesity* **20**, 14-21, doi:10.1097/MED.0b013e32835bc703 (2013).
126 Amireault, P., Sibon, D. & Côté, F. Life without peripheral serotonin: insights from tryptophan hydroxylase 1 knockout mice reveal the existence of paracrine/autocrine serotonergic networks. *ACS chemical neuroscience* **4**, 64-71, doi:10.1021/cn300154j (2013).
127 Troll, J. V. *et al.* Microbiota promote secretory cell determination in the intestinal epithelium by modulating host Notch signaling. *Development (Cambridge, England)* **145**, doi:10.1242/dev.155317 (2018).
128 Roach, G. *et al.* Loss of ascl1a prevents secretory cell differentiation within the zebrafish intestinal epithelium resulting in a loss of distal intestinal motility. *Developmental biology* **376**, 171-186, doi:10.1016/j.ydbio.2013.01.013 (2013).
129 Field, H. A., Ober, E. A., Roeser, T. & Stainier, D. Y. R. Formation of the digestive system in zebrafish. I. Liver morphogenesis. *Developmental biology* **253**, 279-290, doi:10.1016/S0012-1606(03)00308-7 (2003).
130 Stainier, D. Y., Weinstein, B. M., Detrich, H. W., Zon, L. I. & Fishman, M. C. Cloche, an early acting zebrafish gene, is required by both the endothelial and hematopoietic lineages. *Development (Cambridge, England)* **121**, 3141-3150 (1995).
131 Liao, W. *et al.* The zebrafish gene cloche acts upstream of a flk-1 homologue to regulate endothelial cell differentiation. *Development (Cambridge, England)* **124**, 381-389 (1997).
132 Wu, C.-S., Gau, S. S.-F. & Lai, M.-S. Long-term antidepressant use and the risk of type 2 diabetes mellitus: a population-based, nested case-control study in Taiwan. *The Journal of clinical psychiatry* **75**, 31-38- quiz 38, doi:10.4088/JCP.13m08421 (2014).

133 Burcu, M. *et al.* Association of Antidepressant Medications With Incident Type 2 Diabetes Among Medicaid-Insured Youths. *JAMA pediatrics*, doi:10.1001/jamapediatrics.2017.2896 (2017).
134 Noordam, R. *et al.* Selective Serotonin Reuptake Inhibitors Decrease Pancreatic Insulin Secretion in Older Adults and Increase the Risk of Insulin Dependence in Type 2 Diabetes Patients. *The Journal of clinical psychiatry*, doi:10.4088/JCP.15m10048 (2016).
135 Chang, H.-Y. *et al.* Selective serotonin reuptake inhibitor, fluoxetine, impairs E-cadherin-mediated cell adhesion and alters calcium homeostasis in pancreatic beta cells. *Nature Publishing Group* **7**, 3515, doi:10.1038/s41598-017-03747-0 (2017).
136 De Long, N. E., Hyslop, J. R., Raha, S., Hardy, D. B. & Holloway, A. C. Fluoxetine-induced pancreatic beta cell dysfunction: New insight into the benefits of folic acid in the treatment of depression. *Journal of affective disorders* **166**, 6-13, doi:10.1016/j.jad.2014.04.063 (2014).
137 Isaac, R. *et al.* Selective serotonin reuptake inhibitors (SSRIs) inhibit insulin secretion and action in pancreatic β cells. *The Journal of biological chemistry* **288**, 5682-5693, doi:10.1074/jbc.M112.408641 (2013).
138 Da Silva, M. A. *et al.* Antidepressant medication use and trajectories of fasting plasma glucose, glycated haemoglobin, β-cell function and insulin sensitivity: a 9-year longitudinal study of the D.E.S.I.R. cohort. *International journal of epidemiology* **44**, 1927-1940, doi:10.1093/ije/dyv153 (2015).
139 Gehlawat, P., Gupta, R., Rajput, R., Gahlan, D. & Gehlawat, V. K. Diabetes with comorbid depression: role of SSRI in better glycemic control. *Asian journal of psychiatry* **6**, 364-368, doi:10.1016/j.ajp.2013.03.007 (2013).
140 Radojkovic, J. *et al.* Improvement of Glycemic Control in Insulin-Dependent Diabetics with Depression by Concomitant Treatment with Antidepressants. *Medical science monitor : international medical journal of experimental and clinical research* **22**, 2133-2143, doi:10.12659/MSM.899571 (2016).
141 Roopan, S. & Larsen, E. R. Use of antidepressants in patients with depression and comorbid diabetes mellitus: a systematic review. *Acta neuropsychiatrica*, 1-13, doi:10.1017/neu.2016.54 (2016).
142 Maddison, L. A. & Chen, W. Nutrient excess stimulates β-cell neogenesis in zebrafish. *Diabetes* **61**, 2517-2524, doi:10.2337/db11-1841 (2012).
143 Watanabe, H., Rose, M. T. & Aso, H. Role of peripheral serotonin in glucose and lipid metabolism. *Current opinion in lipidology* **22**, 186-191, doi:10.1097/MOL.0b013e3283462273 (2011).
144 Hill, J. H., Franzosa, E. A., Huttenhower, C. & Guillemin, K. A conserved bacterial protein induces pancreatic beta cell expansion during zebrafish development. *eLife* **5**, 18, doi:10.7554/eLife.20145 (2016).

R Core Team. R: A language and environment for statistical computing. (2017). at <https://www.r-project.org/>

Raivo Kolde (2015). pheatmap: Pretty Heatmaps. R package version 1.0.8. https://CRAN.R-project.org/package=pheatmap

Westerfeld, M. *The Zebrafish Book. A Guide for the Laboratory Use of Zebrafish (Danio rerio)*. (Univ. Oregon Press, Eugene, 2007)

CURRICULUM VITAE

Hannah Edelman
Born May 10, 1990 in Minneapolis, MN

EDUCATION

Candidate for Doctor of Philosophy Human Genetics, Johns Hopkins University School of Medicine (Baltimore, MD) *2020 (expected)*
Candidate for Doctor of Medicine Johns Hopkins University School of Medicine (Baltimore, MD) *2020 (expected)*
Bachelor of Arts, Biology with High Honors, Phi Beta Kappa, Swarthmore College (Swarthmore, PA) *2012*

RESEARCH

Doctoral Candidate (2015-present)
Johns Hopkins University School of Medicine, Institute of Genetic Medicine, Laboratories of Dr. Michael Parsons and Dr. Jeff Mumm
Planned and carried out studies investigating the development, differentiation, regeneration, and proliferation of the zebrafish endocrine pancreas. Developed protocols, conducted studies, documented findings, performed data analysis, and interpreted results. Presented findings via poster and oral presentations. Supervised and trained graduate students and lab technicians.

Lab Rotation (*2014-2015)*
Johns Hopkins University School of Medicine, Institute of Genetic Medicine, Laboratory of Dr. Andrew McCallion
Researched the underlying genetic cause of severe craniofacial malformations seen in a patient. Worked with molecular technologies and zebrafish as a model system. Presented findings at local and national meetings.

Lab Rotation (Summer 2013)
Johns Hopkins University School of Medicine, Department of Radiology, Laboratory of Dr. Martin Pomper
Synthesized compounds used for experimental imaging techniques.

Undergraduate Researcher (Summer 2011)(Summer 2010, HHMI Research Fellowship)
Massachusetts General Hospital, Department of Dermatology, Laboratory of Dr. David Fisher
Worked with human cell lines and mouse animal models to research metabolic signaling and drug response in melanoma. Prepared figures for publication.

Undergraduate Researcher (*Summer 2009)*
Vanderbilt University, Department of Biochemistry, Laboratory of Dr. Bruce Carter
Worked with cell lines and rat animal models to research the development of peripheral nerve myelination from Schwann cells.

PUBLICATIONS

W Huang, RL Beer, F Delaspre, G Wang, **HE Edelman**, H Park, M Azuma, MJ Parsons. 2016. Sox9b is a mediator of retinoic acid signaling restricting endocrine progenitor differentiation. *Developmental Biology* 418: 28-39.

X Yang, RC Mease, M Pullambhatla, A Lisok, Y Chen, CA Foss, Y Wang, H Shallal, **H Edelman**, AT Hoye, G Attardo, S Nimmagadda, MG Pomper. 2016. [18F] Fluorobenzoyllysinepentanedioic Acid Carbamates: New Scaffolds for Positron Emission Tomography (PET) Imaging of Prostate-Specific Membrane Antigen (PSMA). *Journal of Medicinal Chemistry* 59: 206-218.

X Yang, NN Yadav, X Song, SR Banerjee, **H Edelman**, I Minn, P van Zijl, MG Pomper, MT McMahon. 2014. Tuning Phenols with Intra-Molecular Bond Shifted HYdrogens (IM-SHY) as diaCEST MRI Contrast Agents. *Chemistry–A European Journal* 20: 15824-15832.

NJ Kaplinsky, SF Gilbert, J Cebra-Thomas, K Lilleväli, M Saare, EY Chang, **HE Edelman**, MA Frick, Y Guan, RM Hammond, NH Hampilos, DSB Opoku, K Sariahmed, EA Sherman, R Watson. 2013. The embryonic transcriptome of the red-eared slider turtle (Trachemys scripta). *PLoS One* 8: e66357.

R Haq, J Shoag, P Andreu-Perez, S Yokoyama, **H Edelman**, GC Rowe, DT Frederick, AD Hurley, A Nellore, AL Kung, JA Wargo, JS Song, DE Fisher, Z Arany, HR Widlund. 2013. Oncogenic BRAF regulates oxidative metabolism via PGC1α and MITF. *Cancer Cell* 23: 302-315.

INVITED SEMINARS

"Serotonergic signaling to the pancreas affects beta-cell proliferation"
(June 2018)
13th International Zebrafish Conference (Madison, WI)

"**Genetic Medicine: Does knowing your genetic "secrets" really impact you?"**
(May 2018)
Lecture as part of the course Medicine: Advances in Health Research and Treatment (with Natalie Beck MGC, CGC and Jacquelyn Britton MGC, CGC)
Osher Lifelong Learning Institute at Johns Hopkins University (Rockville, MD)

"SOX9 regulates epithelial genes in pancreatic progenitors"
(October 2017)
Mid-Atlantic Diabetes Research Symposium (NIH, Bethesda, MD)

"New Directions in Diabetes Treatment: Studying Zebrafish to Stimulate Pancreas Regeneration"
(Sept 2017)
Partnering Toward Discovery series (Johns Hopkins University School of Medicine, Baltimore, MD)

"Serotonergic signaling to the pancreas affects beta-cell proliferation"
(June 2017)
Baltimore Area Zebrafish Monthly Meeting (BALZEE) (IMET, Baltimore, MD)
(May 2017)
Mid-Atlantic Society for Developmental Biology Regional Meeting (UMBC, Baltimore, MD)

"Serotonergic innervation of the pancreas affects beta cell proliferation"
(Dec 2016)
Mid-Atlantic Regional Zebrafish Meeting (NIH, Bethesda, MD)

"*Cbx3* and its role in craniofacial development: zebrafish as a model system for testing dysmorphology candidate genes"
(Nov 2015)
Greenberg Skeletal Dysplasia Clinical Conference (Baltimore, MD)
(Oct 2015)
The American Society of Human Genetics Annual Meeting (Baltimore, MD)
(Oct 2015)
Society for Craniofacial Genetics and Developmental Biology Annual Meeting (Baltimore, MD)

POSTER PRESENTATIONS

"SOX9 ChIP-seq and RNA-seq in PANC-1 cells reveal interesting target genes for pancreatic progenitor biology"
(February 2018)
MD-GEM Genetics Research Day (Johns Hopkins University School of Public Health, Baltimore, MD)

"Serotonergic signaling to the pancreas affects beta-cell proliferation"
(June 2017)
School of Medicine Alumni Student Poster Walk (Johns Hopkins University School of Medicine, Baltimore, MD)
(May 2017)
Department of Surgery Research Day (Johns Hopkins University School of Medicine, Baltimore, MD ***Won Best Student Poster**

"Serotonergic innervation of the pancreas affects beta cell proliferation"

(Sep 2016)
Poster Blitz, Mid-Atlantic Diabetes Research Symposium (NIH, Bethesda, MD)

WORKSHOPS

Human and Mammalian Genetics and Genomics
The Jackson Laboratory (Bar Harbor, ME)
(July 2015)

VOLUNTEER/LEADERSHIP

Herlong Rounds coordinator
(August 2016 - August 2018)
Organized monthly talks by Johns Hopkins Hospital physicians to help MD-PhD candidates keep up with their medical and patient-care knowledge during their graduate school years (Baltimore, MD)

BioEYES volunteer
(Dec 2016)
Helped teach 4th graders at a local elementary school about using zebrafish as a model organism and about the basics of genetics and heredity. *http://www.bioeyes.org*
(Baltimore, MD)

Session Chair
(Dec 2015)
Mid-Atlantic Regional Zebrafish Meeting (Johns Hopkins University School of Medicine, Baltimore, MD)